University of Victoria

Master Thesis

Development of a Finite Element Analysis Workflow for Studying Reverse Total Shoulder Arthroplasty

Supervisor: Dr. Joshua W. Giles

Hooman Shirzadi

(V00927989)

Department of Mechanical Engineering

June, 2021

ABSTRACT

The primary articulation of the shoulder joint is a multi-axis synovial ball and socket joint. By having a loose connection, it provides a wide range of motion; however, this means the joint lacks robustness and is prone to damage most commonly from shoulder dislocations. Rotator cuff tears also cause major problems by limiting the ability to lift the arm into abduction positions. It is common that this insufficiency aggravates arthritis within the shoulder. The study focuses on methods for investigating, describing and quantifying the effects of implant geometric properties on fixation and contact mechanics for a reverse total shoulder arthroplasty implant.

The investigation presents the result of finite element analyses under heavy loading condition on a reverse shoulder implant. These finite element results are validated through comparison to experimental data on the same prosthesis.

The implant is modelled using MIMICS (Materialise, Leuven, BE) and imported into SolidWorks and then ABAQUS (Simulia, Providence, USA) to analyse the distribution of displacement across the scapula. Details of interaction, boundary conditions, loads and material properties are all obtained from research and applied to the model to portray realistic behavior.

The micromotion displacements of the implant were observed in the current study. The models follow the expected trends of the mechanics and what was seen in the experimental data and thus the modeling workflow makes sense overall. This can help to demonstrate the differences between different surgical options (e.g. various reverse implant designs), which may provide a basis from which improved designs can be built and allow more accurate methods to be developed in analyzing shoulder implant effectiveness. However, the method presented here needs further refinement to calibrate the models before it could be utilized in order to answer clinical questions.

Table of Contents

ABSTRACT i
Chapter 1. Introduction and Preliminary information 1
1.1 Introduction 1
1.2 Shoulder Anatomy 1
1.2.1 Bones 2
1.2.2 Joints of the Shoulder Girdle 3
1.2.2.1 The Acromioclavicular Joint 3
1.2.3 Shoulder Joint 5
1.2.4 Muscles, ligaments and tendons 5
1.2.5 Articular Cartilage 7
1.3 Kinematics of the Shoulder 8
1.3.1 Movements of the Shoulder Girdle: 9
1.3.2 Movements of the Shoulder Joint 9
1.3 Shoulder Complex Kinetics 11
1.3.1 Shoulder Joint Forces 11
1.3.2 Shoulder Joint Stabilizers 11
1.4 Prospective Problems in Shoulder 13
1.5 Surgical Cure 14
1.6 Research Hypothesis 14
1.7 Motivation and Objective of the Study 15
1.8 Summary 16
Chapter 2. Literature Review of Reverse Total Shoulder Arthroplasty 17
2.1 Introduction 17
2.2 Shoulder Surgical Treatment 17
2.2.1 Hemi-Arthroplasty 17
2.3.2 Traditional Total Shoulder Arthroplasty 18
2.3.3 Reverse Total Shoulder Arthroplasty 19
2.4 Complications in Surgical Treatment 21
2.4.1 Glenoid Implant Loosening 22
2.4.2 Cause of Loosening 23
2.4.3 Inferior Scapula Notching 23

2.4.4 Dislodgement of the base plate 24
2.4.5 Humeral Side Complications 25
2.5 Finite Element Analysis (FEA) of Shoulder Implant 25
2.6 Conclusion 30
Chapter 3. Methodology and Data Collection 32
3.1 Introduction 32
3.1.1 Body Planes 32
3.2 Methodology 32
3.3 Mechanical Testing Experiment 33
3.3.1 Baseplate 34
3.3.2 Loading Protocol 35
3.4 Simulation 36
3.4.1 Introduction 36
3.4.2 Methodology 38
3.4.3 ABAQUS software 52
3.4.3.2 Finite Element Analysis Technique 53
3.4.3.3 Unit System Within Abaqus 53
3.4.4 Methodology 54
3.5 Summary 58
Chapter 4. Results 60
Chapter 5. Discussion 66
Chapter 6. Conclusion 69
References 70
Appendix A: 74

List of Figures

Figure 1. 1: Shoulder Anatomy- front and back view https://www.animescience101.com/layla-hamilton/shoulder-bones/ 2
Figure 1.2: The left shoulder and acromioclavicular joints (https://mycentralfitness.com) 4
Figure 1.3: Sternoclavicular articulation - Anterior view (..... 5
Figure 1.4: Shoulder joint; and its three degree of freedom (..... 5
Figure 1.5: Glenohumeral Ligaments 6
Figure 1.6: Rotator cuff muscles (..... 7
Figure 1.7: Glenoid labrum tear (https://orthoinfo.aaos.org/en/diseases--conditions/shoulder-joint-tear-glenoid-labrum-tear) 8
Figure 1.8: Shoulder Range of Motion 10
Figure 1.9: Resultant force of external rotation (X), neutral (N), and internal rotation (I) vectors. 12
Figure 1.10: Normal, V-shaped widening, Moderate subluxation, Advanced subluxation and dislocation definitions 12
Figure 2.1: Shoulder Hemi-Arthroplasty 17
Figure 2.2: A 70-year-old woman who underwent a left total shoulder arthroplasty 18
Figure 2.3: A 79-year-old woman who underwent hemi-arthroplasty of the left (McFarland et. al.) 18
Figure 2.4: Left: Universal Arrow System, right: Inbuilt medial notch on humeral cup (Katz et al.) 21
Figure 2.5: Scapular notching (http://shoulderarthritis.blogspot.com/2017/04/scapular-notching-is-it-about-notch-or.html) 24
Figure 2.6: base plate dislodgment 25
Figure 2.7: Finite element model of the Reverse Shoulder Prosthesis (Nazeem et al., 2007) 26
Figure 2.8: finite element models of: (a) Anatomical (Zimmer); (b) Bayley–Walker(Stanmore); (c) Delta III (Depuy); (d) RSPneutral (Encore); (e) RSP-reduced (Encore); (f) Verso (Biomet) 27
Figure 2.9: 2D finite element reverse shoulder model and its boundary (Yang et al. 2013) 28
Figure 2.10: Lateralization models. (A) No lateralization, (B) Lateralization via bone graft, (C) Metallic lateralization via the baseplate, (D) Metallic lateralization via the glenosphere. (Dennard et al. 2016) ... 29
Figure 3.1: Body planes 32
Figure 3.4: Mimics modules (Mimics tutorial) 39
Figure 3.5: Axial (top right), sagittal (bottom left) and coronal (top left) views of the scapula 40
Figure 3.6: Dialogue box for setting the thresholding 41
Figure 3.7: Purple mask assigned to the scapula 42
Figure 3.8: Mimics, icon for region growing function 43
Figure 3.9: Export steps of STL files 44
Figure 3.18: Mesh convergence analysis 51

Chapter 1. Introduction and Preliminary information

The clinical nature of this project has necessitated the* use *of some medical terms throughout the text. A glossary of terms has been Added to assist the reader, as Appendices A.

1.1 Introduction

Nowadays, human motion analysis is one of the most important research fields. To determine the best course of treatment in surgeries or rehabilitative therapy, the results of human motion analysis are used to positively affect the medical community. Furthermore, the results assist in designing better orthotic and prosthetic devices and equipment. Also, these kinds of analyses are utilized in some sport fields for athletic and strength training purposes.

The most unconstrained part in a body is the shoulder joint which plays a crucial role in the mobility of the arm segment. Moreover, lots of daily activities and movements depend on the mobility and agility of the arms and therefore if any problem happens for the function of the shoulder it will directly adversely affect the body movement.

The aim of this chapter is to briefly describe shoulder anatomy with its bones, articulations, and soft tissues. Also, the shoulder kinematics and the different range of motion will be discussed. Afterwards, shoulder joint diseases and the suggested surgical procedures are mentioned. At the end, the aim of this project and the research hypothesis is discussed. It is crucial to understand the former mentioned points owing to the fact that they directly affect the readers' understanding of the study.

1.2 Shoulder Anatomy

The shoulder girdle has several bony joints (articulations), which connect the segments to each other. The important ability of the shoulder joint is its large range of motion which is crucial for conducting many daily activities. (Figure 1)

1.2.1 Bones

The shoulder girdle consists of three bones which are the Clavicle (collarbone), and the Scapula shoulder blade. Moreover, the Humerus (upper arm bone) and scapula create the shoulder joint.

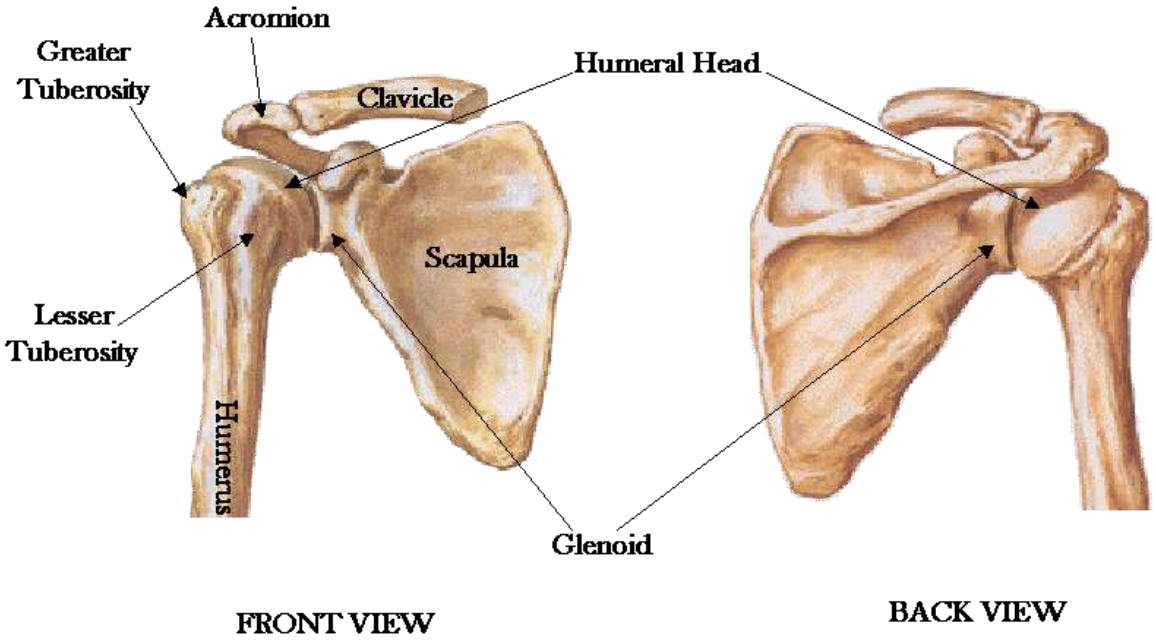

Figure 1. 1: Shoulder Anatomy- front and back view https://www.animescience101.com/layla-hamilton/shoulder-bones/

1.2.1.1 The Clavicle:

The clavicle, or collarbone, is a long bone that serves as a strut between the shoulder blade and the sternum (breastbone). There are two clavicles, one on the left and one on the right. The clavicle is the only long bone in the body that lies horizontally. The medial half of the bone is anteriorly convex and the lateral side is concave (Hay & Reid, 1999; Roetert, 2003).

1.2.1.2 The Scapula:

The scapula is a flat bone that is roughly triangular in shape with a medial, lateral and superior border (Hey & Reid, 1988). In anatomy, the scapula (plural scapulae or scapulas), also known as the shoulder bone, shoulder blade, wing bone or blade bone, is the bone that connects the humerus (upper arm bone) with the clavicle (collar bone). Like their connected bones, the scapulae are paired, with each scapula on either side of the body being roughly a mirror image of the other. The lateral aspect of scapula, the glenoid, acts as a flexible ball-and-socket joint which meets the head of the humerus to form a glenohumeral cavity. (Figure 1)

1.2.1.3 Humerus:

The humerus is the long bone in the upper arm. It is articulated between the shoulder blade (glenohumeral joint) and the elbow joint (radius and ulna). The face of the glenoid and head of the humerus create the joint cavity which is covered by articular cartilage.

1.2.2 Joints of the Shoulder Girdle

The shoulder girdle consists of three separate joints: the acromioclavicular, glenohumeral, sternoclavicular, and scapulothoracic, along with many tendons, ligaments, and muscles that work in concert to manipulate the arm.

1.2.2.1 The Acromioclavicular Joint

The acromioclavicular joint is a plane type synovial joint. It is located where the lateral end of the clavicle articulates with the acromion of the scapula.

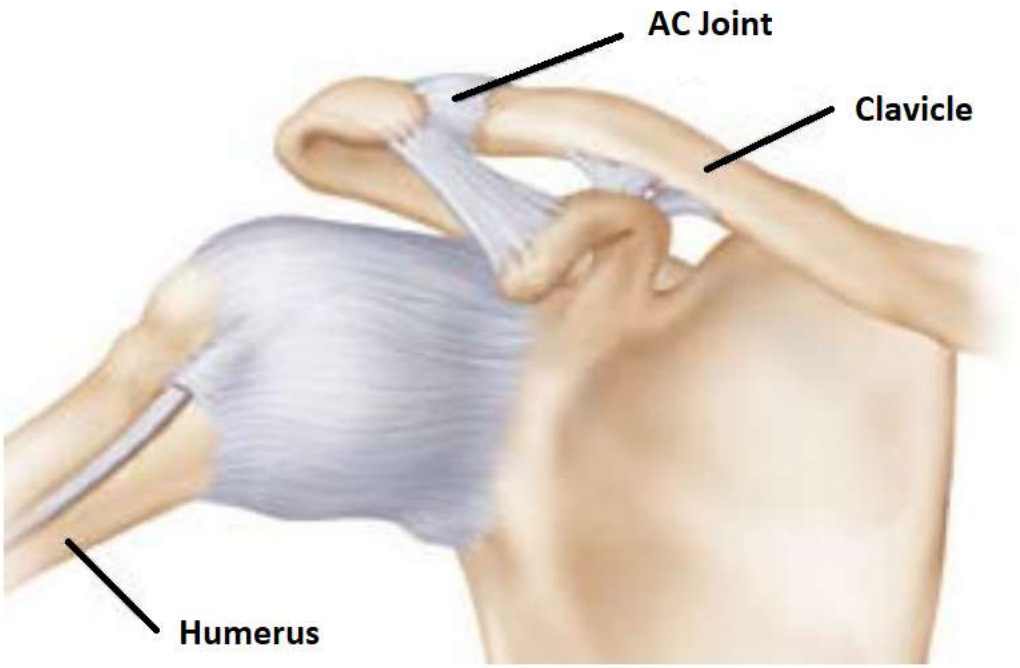

Figure 1.2: The left shoulder and acromioclavicular joints (https://mycentralfitness.com)

The superior and the inferior acromioclavicular ligaments helps in supporting this joint (Marieb, 1995; Hay & Reid, 1999). One of the ligaments named coracoclavicular, which is not part of the joint, helps to maintain the integrity of the joint. One of the most common sport injury is dislocation of this joint when the athlete falls on his/her shoulder which this kind of injury usually referred to as a "shoulder separation" incorrectly. (Hamill & Knutzen, 1995; Hay & Reid, 1999; Martini et al., 2001).

1.2.2.2 The sternoclavicular Joint

The sternoclavicular joint is a synovial joint between the manubrium of the sternum and the clavicle bone. A fibrous capsule covers the articulation and provides strength to the joint by an anterior and posterior sternoclavicular ligament, interclavicular ligament, and a costoclavicular ligament (Marieb, 1995; Hay & Reid, 1999). This kind of joint is a strong joint so the dislocation of it is uncommon. It is likely that the clavicle may break when the hand strikes the ground on falling. However, it won't adversely affect the joint like cause dislocation (Hay & Reid, 1999; Martini et al., 2001).

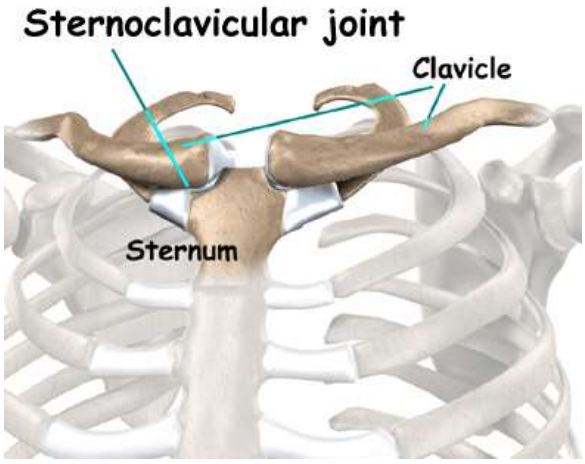

*Figure 1.3: Sternoclavicular articulation - Anterior view (*https://eorthopod.com/sternoclavicular-joint-problems/*)*

1.2.3 Shoulder Joint

The shoulder joint or glenohumeral joint is a ball-and-socket type of joint, formed by the small, shallow, pear-shaped glenoid cavity of the scapula and the head of the humerus (Figure 4) (Marieb, 1995). In ball-and-socket joints, the hemispherical or spherical head of one bone articulates with the concave socket of another bone. These joints' type is multi-axial with universal movement in all axes and planes.

Figure 1.4: Shoulder joint; and its three degree of freedom (https://pivotalphysio.com/three-common-shoulder-injuries/*)*

1.2.4 Muscles, ligaments and tendons

Shoulder bones are held together by its muscles, ligaments, and tendons. Ligaments (which attach bone to bone) and tendons (which attach shoulder muscle to bones) provide more stability and strength for the shoulder joint.

As it is illustrated in (Figure 5), the Glenohumeral ligaments positively affect the joint stability and prevent translation of the head of the humerus from the glenoid fossa.

The stability of the shoulder joint is provided by its muscles and tendons which is known as the shoulder dynamic stabilizers as shown in Figure 5.

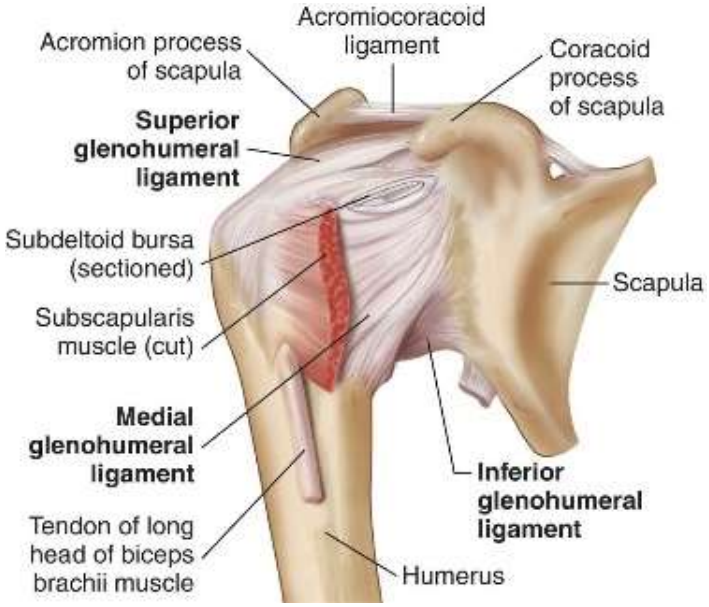

Figure 1.5: Glenohumeral Ligaments (https://medical-dictionary.thefreedictionary.com/)

They cover the humeral head and help it to be into the glenoid fossa, the movement and stability of the shoulder complex is provided by the muscles. In some activities for instance lifting certain muscle groups help to move the shoulder while some of them provide the stability of the joint. The rotator cuff muscles are: supraspinatus, subscapularis, infraspinatus, teres minor. Also, the dynamic muscle stabilizers are the deltoid, long head of the biceps tendons, and teres major. In the midrange of the shoulder joint motion the dynamic support is provided because of the humeral head compression in the glenoid cavity. Each muscle of the shoulder has its own duties. For instance, the subscapularis muscle provides anterior stability, the posterior rotator cuff muscles provide posterior stability, the long head of the biceps brachii actually prevents superior and anterior humeral head translation, and the other scapulothoracic muscles and deltoid keep the scapula stable to provide maximum glenohumeral stability. The other job of these muscle group is rotation and depression of the humeral head when the arm elevates to keep the humeral head in its position.

The capsule, glenoid labrum, and ligaments, provides the shoulder with static stability. These stabilizers are acting together to provide complex and also smooth motion simultaneously. The rotator cuff muscles are shown in figure 6. These muscles define the shoulder state and range of motion. Although the ball and socket articulation is delicate, it is reliable to provide a wide range of motion for the shoulder complex. Overall, shoulder stability is provided by both static and dynamic components, which provide maintenance of the humeral head in the glenoid fossa.

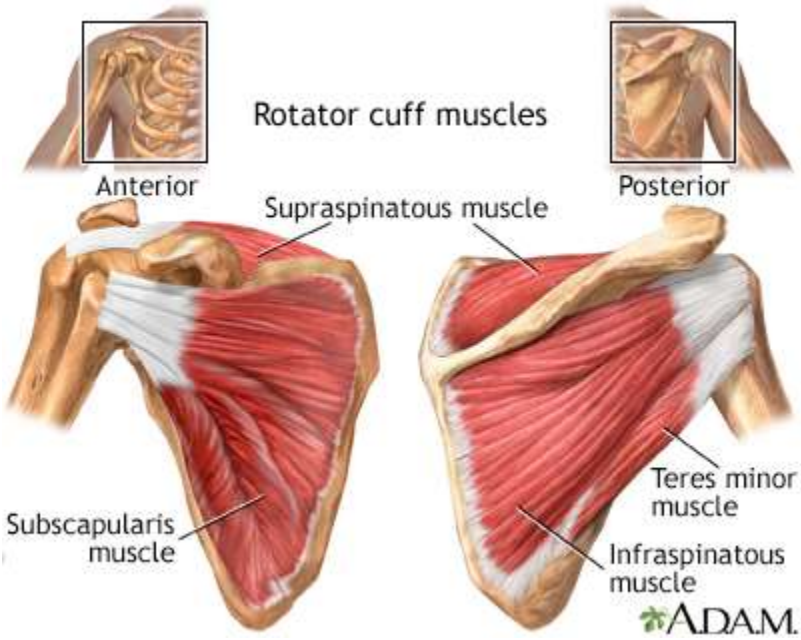

Figure 1.6: Rotator cuff muscles (https://medlineplus.gov/ency/imagepages/19622.htm)

1.2.5 Articular Cartilage

Articular cartilage covers the proximal humerus and face of the glenoid and also protect the joint cavity. Figure 7 illustrates the glenoid labrum tear which shows the correspondent cartilage structures.

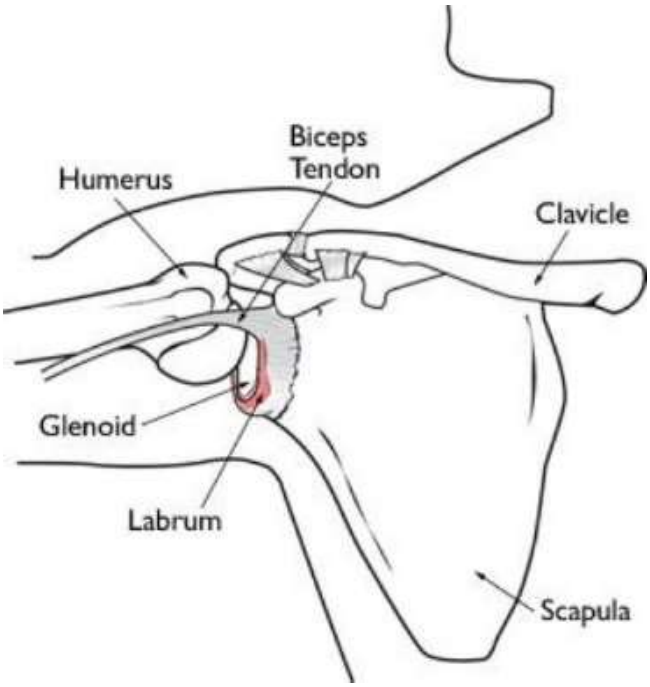

Figure 1.7: Glenoid labrum tear (https://orthoinfo.aaos.org/en/diseases--conditions/shoulder-joint-tear-glenoid-labrum-tear)

The labrum is the cup-shaped rim of cartilage that lines and reinforces the ball and socket joint of the shoulder, which is comprised of the glenoid (the shallow shoulder socket) and the head, or ball of the upper arm bone known as the humerus. The labrum is the attachment site for the ligaments and supports the ball and socket joint along with the rotator cuff tendons and muscles. It contributes to shoulder stability and, when torn, can lead to partial or complete shoulder dislocation.

Cartilage consists of extracellular matrix, produced by chondrocyte cells that are sparsely distributed homogenously throughout the matrix. This matrix is consisting of some interwoven collagenous fibrils and also ground substance which form the glue to the fibrous network. Actually, there are no nerves and vascular supply within the cartilage except at the bone/cartilage interface. 70% of the matrix is water, however, the characteristics of the bearing material is attributed to the mucopolysaccharides.

1.3 Kinematics of the Shoulder

Kinematics is a branch of classical mechanics that describes the motion of points, bodies (objects), and systems of bodies (groups of objects) without considering the forces that cause them to move. The human movements restriction or their inability to move might adversely affect their

susceptibility to musculoskeletal injury. The shoulder is very unstable and also the most movable and complex joint in the body. This joint is easily injured by simple overuse, impact, or lifting heavy objects and heavy workout. In the following sections the shoulder kinematics will be discussed and reviewed.

1.3.1 Movements of the Shoulder Girdle:

The scapula movements depend on the combination of both the sternoclavicular and the acromioclavicular joints motions. The sternoclavicular and acromioclavicular joint permits movement in almost all directions and the gliding motion of the articular end of the clavicle on the acromion, and also some rotation of the scapula both forward and backward on the clavicle, respectively (Hay & Reid, 1999).

The combination movements of the scapula and clavicle are as follows:

1.3.1.1 Adduction and Abduction:

Abduction of the scapula occurs when the medial border moves away from the spine. Adduction of the scapula occurs when the medial border of the scapula moves toward the spine. Though, adduction can be seen when sticking out the chest and pulling back the shoulders (Yokochi et al., 1989; Hay & Reid, 1999).

1.3.1.2 Elevation and Depression:

The downward movement of the scapula is called depression and elevation occurs when the scapula moves upward without any rotation as one raise his shoulder. Depression and elevation could be felt by placing the hand on the scapula and the clavicle simultaneously or separately while first lifting the shoulders and then pushing them down again (Yokochi et al., 1989; Hay & Reid, 1999).

1.3.1.3 Rotation:

The axis of rotation could be at the acromioclavicular or the sternoclavicular joint. Downward rotation is the inward and downward movement of the scapula inferior angle. Upward rotation is the outward and upward movement of the inferior angle of the scapula.

1.3.2 Movements of the Shoulder Joint

The movements of the glenohumeral joint and the shoulder girdle usually occur together and should be considered together however, they are not the same. Flexion, extension, abduction, adduction, a slight degree of hyperextension, circumduction, medial and lateral rotation might all

occur at the shoulder joint, however, their range of motion is restricted if the shoulder girdle is not involved (Hay & Reid, 1999) (figure 8). When the flexion and abduction is happening the glenohumeral joint moves at the same time. In the first 30 to 60 degree of abduction, scapula remains fixed. After 30 degree of abduction and 60 degree of flexion, a constant relationship between the humeral and the scapula movement exists so that for every one degree of scapular rotation there will be two degrees of humeral movement (Yokochi et al., 1989; Hay & Reid, 1999).

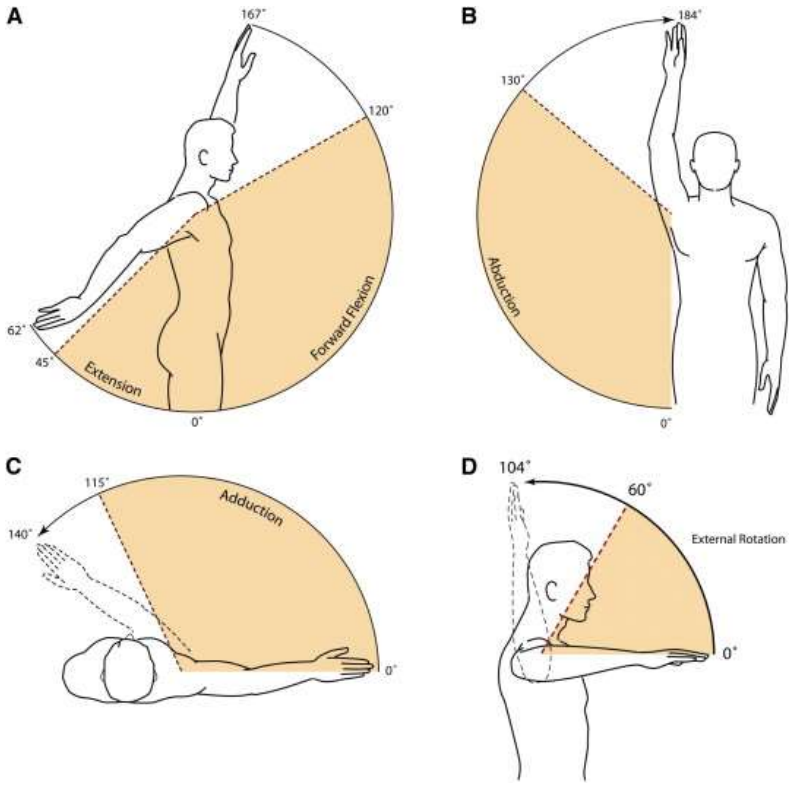

Figure 1.8: Shoulder Range of Motion (S. Namdari et al.)

The full range of motion in flexion of the arm above the head could be merely conducted if medial rotation of the humerus occurs, however, full abduction is possible from this position (Yokochi et al., 1989). The range of motion is restricted to approximately 90 degrees if abduction is attempted with the hand palm facing the thigh. From this point, lateral rotation will permit further abduction (Hay & Reid, 1999).

Shoulder range of motion could be varied depending on the joint degree of freedom. Shoulder complex has six degree of freedom as follows: flexion, extension, abduction, adduction, internal rotation (with arm abducted) and external rotation (with arm abducted).

Knowing how bony and soft-tissue components of the shoulder complex interact with each other or with an endo-prosthesis to generate movement is very important because for instance, the movement at the glenohumeral joint requires motion at the other shoulder joints. The scapulo-humeral rhythm is known as the coordinated movement between two shoulder joints. This term describes the movement that occurs at the glenohumeral joint compared to movement that occurs at the other shoulder complex joints. For example, the acromioclavicular, the sternoclavicular, and the scapulothoracic joints. The scapulothoracic joint is not a main joint however, it shows the movement of the scapula against the thoracic wall during the arm movement. On the other hand, the scapulo-humeral rhythm allows the shoulder to move through its full range of motion and also the head of the humerus to be centered in the glenoid cavity. There were some studies and experiments that reveal for every 180 degrees of shoulder abduction, 120 degrees occurs at the glenohumeral joint and 60 degrees occurs at the scapulothoracic joint but for every 15 degrees of shoulder abduction, 10 degrees occurs at the glenohumeral joint and 5 degrees occurs at the scapulothoracic joint. If anything happens to the scapula-humeral rhythm the humeral head does not remain centered which could adversely affect the shoulder complex efficiency and may the rotator cuff tearing and tendonitis happens. However, in a normal case, the shoulder motion is a motion of the mentioned muscles/joints working with each other to conduct the known range of movements.

1.3 Shoulder Complex Kinetics

Shoulder joint kinetics has complex behavior. In this section the internal created forces will be categorized and the mechanism of this joint will be described.

1.3.1 Shoulder Joint Forces

As it is illustrated in Figure 9 the muscles generate the maximum force through the glenohumeral joint at 90 degree of abduction.

1.3.2 Shoulder Joint Stabilizers

Dynamic, passive and active stabilizers are the mechanisms that help stabilize the joint (Matsen III et al. 2006). The mechanisms of stabilization in the shoulder joint are the glenoid conformity/concavity, capsule-ligamentous restraints, muscular compression, adhesion-cohesion of the articulation surfaces and suction. There is a difference between subluxation and dislocation. Dislocation is defined as the point when rim edge aligns with the head center. However,

subluxation is defined as the point when the resultant joint force falls beyond the joint rim edge (Figure 10).

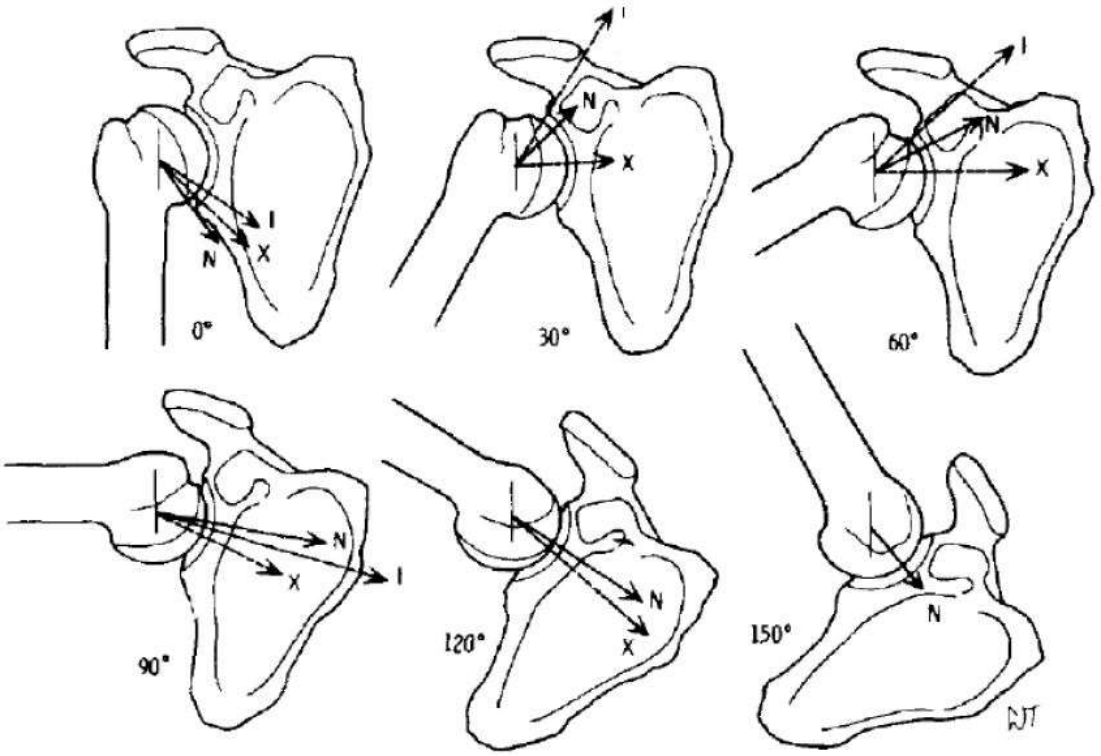

Figure 1.9: Resultant force of external rotation (X), neutral (N), and internal rotation (I) vectors. (Fu et al. 1991)

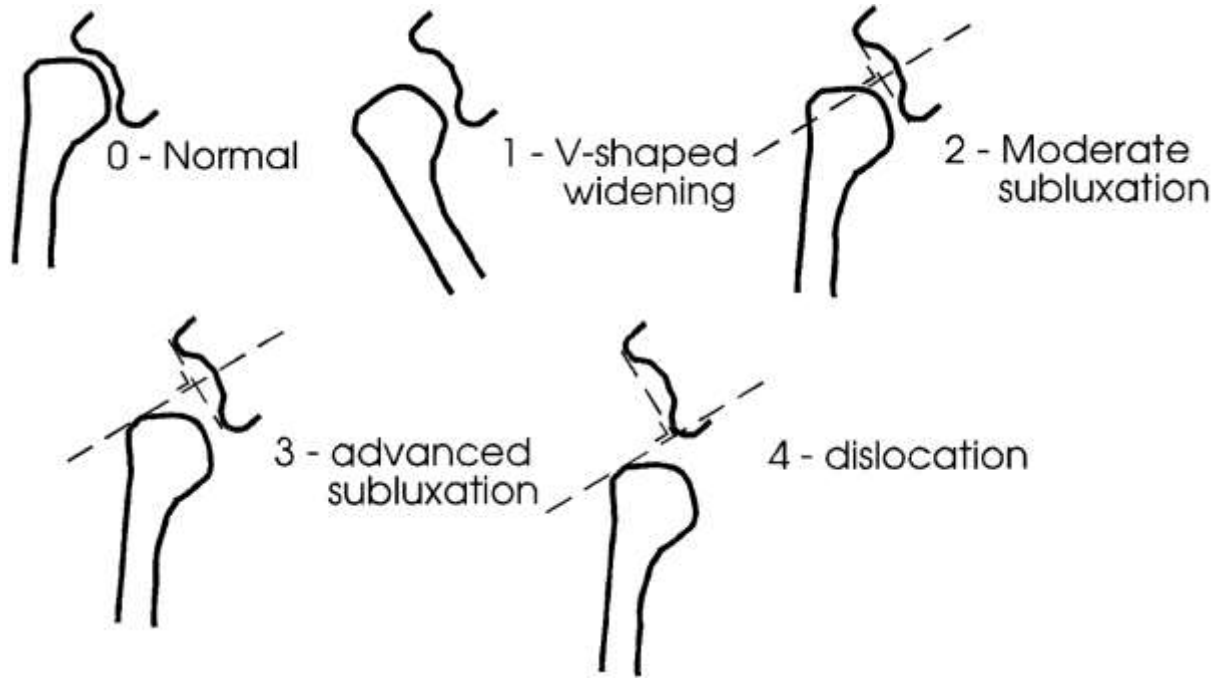

Figure 1.10: Normal, V-shaped widening, Moderate subluxation, Advanced subluxation and dislocation definitions (https://www.ahajournals.org/doi/10.1161/01.STR.30.5.963)

Joint stability is affected by the level of glenoid concavity and conformity in two ways; depth will increase the transverse force required to subluxate or dislocate the joint or increasing either the glenoid conformity. Similarly, increasing the compressive perpendicular force from surrounding muscular tissues increases the transverse force needed to destabilize the joint. Also, the flexibility of the labrum allows for small head movement in the ball and socket joint. (Matsen III et al. 2006).

Shoulder complex has four rotator cuff muscles which they provide compression force and also stability around the joint both actively and passively. The supraspinatus is the main superior stabilizer, the infraspinatus and teres minor, both provide the main posterior support. The subscapularis is the primary stabilizer for anterior aspect of the joint. Other shoulder complex muscles help to provide compression as well, however, their support are more effective at different positions during the joint movement. One of the rotator cuff duties is to provide the mid-range stability of the shoulder complex and also throughout all movements of the shoulder. The second duty for rotator cuff muscles is to act as agonists and antagonists in shoulder motion (Chadwick et al. 2004).

The joint capsule and ligaments limit the humeral head range of movement so they prevent damages to the tissues. Thereby, the ligaments stay lax and unloaded during mid-range movement where the muscular forces dominate (Labriola et al. 2005; Matsen III et al. 2016; Schiffern et al. 2002). The forces exerted by the muscles decrease and are no longer sufficient to provide stability, as the shoulder reaches its limit. So, the capsule and ligaments become effective and stretch in tension, preventing further movement, and creating a reactionary force applied to the head. Which this capsuloligamentous mechanism is passive and despite of the muscles does not require energy to act.

Another shoulder complex mechanism is adhesion-cohesion. The adhesion-cohesion is the smooth sliding of the glenohumeral joint because of the thin film of synovial fluid between the articulating tissues which allow sliding and resist separation. The suction is created between the head and glenoid socket due to the conformity and concavity (radial match) provided by the labrum, generating low pressure in the joint, which maintains the glenohumeral contact.

1.4 Prospective Problems in Shoulder

The normal shoulder complex is a ball and socket joint. the socket is called the glenoid and the ball is called the humeral head. In the arthritic shoulder the normal cartilage (smooth surface of

joint) is worn away and there is bone-on-bone contact without the normal smooth gliding surfaces, which are able to glide on each other with little friction and wear. The joint might also become irregular from bony growth (named osteophytes), which is the body's attempt to "heal" the cartilage injury. When the irregular joint surfaces have contact with one another and rubbing on each other because of the inflammation of wear, the patient feel the pain in that area.

One of the predicaments regarding to the shoulder movement at the glenohumeral joint area is arthritis which is basically the erosion of the solid cushioning known as cartilage and the lubricated synovium causes the bones to rub together when moving. Usually, two types of arthritis happen in the shoulder joint. The first one is osteoarthritis which is a common occurrence caused by constant exposure of the joint to high stresses. The second type is called rheumatoid arthritis which it occurs when the synovium enflames destroying the bone and cartilage it encompasses. Also, when the rotator cuff muscles tears happening, the patients cannot utilize their shoulder complex properly. To solve the problem, surgeons usually conduct some arthroplasty surgery (Labriola et al. 2005; Matsen III et al. 2016; Schiffern et al. 2002).

1.5 Surgical Cure

Total replacement arthroplasty the surgical method to cure arthritis is a specific form of orthopaedic surgery. In this type of surgery, the ends of the joints are cut off and replaced with an implant. In total shoulder replacement this involves replacing the head of the humerus with a metal hemisphere and the glenoid fossa in the scapula with a polyethylene cup. One of the main flaws of this method is that it will not fully restore function if the patient had any musculoskeletal problems before the surgery, which were not due to the geometry of the joint but to the supportive muscles. Specifically, when that limitation is caused by a loss of strength, or tear of the rotator cuff muscles.

1.6 Research Hypothesis

Conducting finite element analysis (FEA) is one of the methods for investigating the stresses and micro-motions in the implant components and shoulder bone. This method has already been utilized for comparing a healthy and arthritic shoulder joint (Büchler et al.). They concluded that

the stress is evenly distributed in a healthy scapula; whereas the stress distribution in the arthritic shoulder are highly localized.

One of the newly approved implants in Canada is the reverse total shoulder arthroplasty that has been utilized successfully for over twenty years in Europe. In March of 2004, the FDA approved it for use in the USA. This kind of implant has lots of benefits for patients that have their rotator cuff muscles torn or in some complex case of fractures. In the reverse total shoulder arthroplasty implant a glonoid sphere component is located at the glonoid cavity and the humeral cup is located at the proximal humerus which is the opposite side of the traditional shoulder arthroplasty or a normal shoulder. This kind of implant design has the biomechanical effect of translating the center of the rotation medially. This feature causes the deltoid to have a larger moment arm and enables more shoulder range of motion and abduction despite nonfunctional rotator cuff muscles and also when there is a significant bone loss. Thereby, the thesis hypothesis is that an improved Finite Element Model of Reverse Total Shoulder Arthroplasty could enable us to improve our understanding of the implants mechanics, fixation, and modes of failure.

1.7 Motivation and Objective of the Study

The project objective is to examine the mechanical behavior of the glenoid interface of a shoulder fitted with a certain RTSA implant by utilizing finite element analysis and comparing the simulated results to existing experimental data taken when the joint was subjected to high loading. Results will demonstrate how the RTSA implant reacts to realistic loading and will help to validate the developed finite element modeling method. Finite element method will be utilized because it is an easily accessible method and will be able to show all the stresses and micro-motions that occurs within a relatively small, inaccessible bone and implant parts such as graft and base plate.

The results the developed finite element model could produce may be helpful in predicting areas where the stress concentrations can cause failure to either the bone or prosthesis. Additionally, the results could eventually be used to guide the design or development of future RTSA implants.

Also, based on the results of this thesis, using a patient CT-scan images, one can develop and design a RTSA implant for those patients. Considering the age and the physical characteristics of the patients, an implant can be optimized regarding its weight and high strength. Therefore, a

RTSA implant could be made as patient specific; it means that according to the patients' scapula physical characteristics, the implant will be designed.

This thesis is divided into three main sections: background, finite element modelling, experimental validation. The first section (background) includes the second and third chapters and covers the background and literature review.

1.8 Summary

The chapter discussed at first the shoulder anatomy, kinematics and demonstrated the range of normal movement of the shoulder joints. Moreover, the shoulder problems were presented and also surgical solution for fixing the problems were highlighted. The objective of the thesis is to conduct and validate finite element analyses of RTSA in order that the model could be used int eh future to better understand the loading mechanics under various conditions and potentially improve implant design.

In the next chapter a total review for traditional and reverse total shoulder arthroplasty and also the main finite element analysis studies that have been done in this area will be discussed.

Chapter 2. Literature Review of Reverse Total Shoulder Arthroplasty

2.1 Introduction

This chapter will present the common shoulder problems and the surgical treatments briefly. Also, the mechanical analysis that previously conducted done by other researchers in the area of reverse total shoulder arthroplasty has been presented in this chapter.

2.2 Shoulder Surgical Treatment

There are three main types of shoulder replacement (hemi-arthroplasty, traditional total shoulder arthroplasty, reverse total shoulder arthroplasty), the clinical indications for using each are unique as outlined in the sections below

2.2.1 Hemi-Arthroplasty

Hemi-arthroplasty is a surgical procedure that replaces one half of the shoulder joint. The humeral head is replaced with a prosthesis and the glenoid (socket) is left intact (figure 2).

Figure 2.1: Shoulder Hemi-Arthroplasty (https://www.medeguru.com/orthopedics/partial-shoulder-replacement-surgery/)

When the doctor determines that only the humeral side of the joint (ball) should be resurfaced, researchers call this a partial shoulder replacement or hemi-arthroplasty.

2.3.2 Traditional Total Shoulder Arthroplasty

This kind of surgical treatment involves replacing the proximal humerus (humeral head) and the glenoid cavity. A traditional total shoulder arthroplasty might be the best option when the rotator cuff muscles are not damaged and just the glenoid cavity is damaged.

In traditional shoulder replacement surgery, the painful surfaces of the damaged shoulder are resurfaced with artificial shoulder parts. The part that replaces the glenoid cavity is made up of a smooth plastic concave shell that matches the round head of the ball and the part that replaces the ball consists of a stem with a rounded metal head which makes the humeral head. When the two side of the joint, the glonoid cavity and the proximal humeral head are resurfaced, researchers name it as total shoulder replacement. Figure 2 illustrates a 70-year-old woman who underwent a left total shoulder arthroplasty because of the corrosive arthrosis which is showing a standard total shoulder arthroplasty (the glonoid cavity and the proximal humerus are changed). Figure 3 shows a 79-year-old woman who underwent hemi-arthroplasty of the left shoulder. In this surgery the left proximal humeral head was replaced by the implant.

Figure 2.2: A 70-year-old woman who underwent a left total shoulder arthroplasty

Figure 2.3: A 79-year-old woman who underwent hemi-arthroplasty of the left (McFarland et. al.)

2.3.3 Reverse Total Shoulder Arthroplasty

When the rotator cuff muscle tear happens in a person, surgeons usually conduct arthroplasty surgery using reverse total shoulder arthroplasty surgical treatment. The traditional shoulder arthroplasty would not be helpful for these patients because in TSA there will be less congruency between the glenoid cavity and humeral cap and the patient needs to apply more force with the rotator cuff muscles which are already torn. The shoulder is a ball-and-socket joint. In a normal shoulder, the proximal humerus (upper arm bone) is in a ball shape. The ball fits into a socket (glenoid cavity) formed by the scapula (shoulder blade). The ball and socket form the shoulder joint. In reverse total shoulder arthroplasty, the glenoid sphere is located at the glenoid cavity and the humeral cap is placed at the proximal humeral head so the ball and socket are reversed compare to the traditional total shoulder arthroplasty. It has a biomechanical effect; the center of the rotation is translated medially in RTSA so that the moment arm of the deltoid muscle would be increased and it positively affect the muscles' function. However, it increases the impingement of the joint. The most common impingement that happen in shoulder joint is scapular notching. It is because of unwanted contact between the polyethylene component of humeral cap and the bone of the scapula.

2.3.3.2 Grammont's Prosthesis 1985

Grammont presented two reverse implant designs. The first model of Grammont is characterized by in two elements (Katz 2007). The first part was the glenoid component which formed from two-thirds of a sphere and was actually connected to a glenoid base prepared with a bell-shaped saw. The second part was the polyethylene humeral head and the articulating part had a concavity corresponding to one-third of a sphere. Grammont had utilized this implant on eight patients. In this implant model because of the laterality of the center of rotation position of the glenoid component the shear force would be increased so Grammont had to develop his design and redesign his first model.

The modified design was produced in 1991. In the second generation the periphery of the metaglenoid was conical and smooth with a Morse-Taper effect and also the metaglenoid was coated with hydroxyapatite on its deep surface to improve bony fixation. In this design the polyethylene cup (a third of a sphere) was fitted over the epiphyseal end. However, the size of the cup was insufficient and rapidly deteriorated as a result of medial impingement.

2.3.3.3 Post-Grammont

De Wilde et al., Frankle et al. and Harman et al. explained several new implant models based on the experiences. Tornier Company designed an implant which incorporates the bio-mechanical principles described by Grammont, but with some new innovations compare to Grammont design. In their model the locking screws were divergent which they fix the metaglenoid. The reason they add divergent screws was it adds strength to the joint. They argue that it adds strength but there are not clear publications in this regard. Nyffeler et al. recommended that in the Tornier design, the metaglenoid could be installed lower on the glenoid with a bit more inferior tilt. Also, Frankle et al. reported an implant design that placed less medially compare to the former designs and also its center of rotation was closer to a regular normal anatomical location. The total range of motion in this type of design was improved compare to the other models but the abduction was less than the former designs. They concluded that a concave metaglenoid showed a better result in terms of fixation compare to a flat one. It is concave on its medial side where it contacts bone.

The inferiorly extension of the glenosphere avoids the Duocentric (A third-generation prosthesis called the Duocentric prosthesis in 2003) prosthesis design from medial impingement. This model obeys the Grammont principles so in this model the center of rotation lied at the level of the glenoid.

In 2007, Katz et al. designed the “universal arrow system” to improve the range of motion after the surgery and also to eliminate the medial impingement risk (figure 4).

Figure 2.4: Left: Universal Arrow System, right: Inbuilt medial notch on humeral cup (Katz et al.)

In this design the center of rotation is the glenoid, however the design allows the prosthesis to be placed less medially compare to former designs. To avoid friction against the pillar of the scapula, the humeral cup has the inbuilt medial notch.

DeWilde et al. conducted experiment and they concluded that medialization and lowering the implant positively affect the moment arm of the deltoid and it actually improves the arc of rotation. This feature is significantly important in daily activities performing. Valenti et al. followed-up the patients that had undergone the arrow system for twelve months and they concluded that the arrow series did not show any signs of scapular notching or glenoid loosening.

2.4 Complications in Surgical Treatment

Many of issues that might happen to the patient during or after the surgery is related to medical situation and it cannot be prevented from happening. These problems are such as infection,

stiffness (which usually happens for the patients after the surgery and could be resolved by physical therapy and time), component loosening (include growing bone into implant which cause implant dislocation and can occur years after surgery), fracture (when the implant components are inserting to the glenoid or humerus, they could crack the bones), nerve injury (this type of surgery could adversely affect one's arm or shoulder nerve system; it happens rarely), blood clots could happen for patients' upper extremity after the surgery. The main danger of blood clots is when they dislodge and travel to patients' veins in their lungs. This phenomenon is called a pulmonary embolus and could result in chest pain, respiratory difficulties, or even death), bleeding (excessive bleeding occurs after or during the surgery if the blood vessels around the shoulder are damaged; it happens rarely), osteolysis (which is the body's response to the plastic wear debris from the shoulder replacement. The human body is prone to absorb the plastic particles and makes the bone around the shoulder joint weaken), dislocation, need for further surgery (shoulder replacements occasionally fails sooner than expected; it is uncommon in this kind of surgery), death (it is because of heart problems that arise or worsen after surgery or as mentioned above due to blood clots travelling through the body to the lung or even lots of bleeding during or after the surgery). However, there are some other issues such as failure, fracture, loosening, and dislocation of the joints that could be prevented from happening by conducting simulations through finite element analysis and developing the implant design which are directly related to the current study objective.

Biomechanical complications of the shoulder surgery that are related to the current project are as follows:

2.4.1 Glenoid Implant Loosening

Hill et al. followed up 14 patients after an average of 5.8 years and they concluded than nine patients (64%) had a good satisfactory outcome whereas 5 (36%) of the patients were unsatisfactory with 2 (21%) failing because of the glenoid loosening, requiring re-surgery. Martin et al. showed TSA failure occurred in 16 out of 140 shoulders (11%) and 5 of them were because of the loosening of the glenoid implant. Wallace et al., conducted a study and found out that out of 86 shoulders, 14 showed complications (16%) with 8 (9%) requiring revision, but loosening was not a cause for re-surgery. Scarlat et al. investigated 37 retrieved implants. They found the cause for re-surgery for 95% (18/19) of the glenoid were because of the instability and loosening.

2.4.2 Cause of Loosening

Regarding the loosened and retrieved glenoid there are a few studies. However, there are some papers that have investigated these areas. For instance, Wirth et al., Yian et al., and Nyffeler et al. investigated the area of failure which most of them have focused on the surface wear. There are some clinical studies in this area as well. Bohsali et al. and Matsen et.al utilized radiolucent lines (r. lines) as a loss of fixation by considering either the formation of fibro-cartilage tissue or physical interfacial gap to indicate glenoid loosening as a bone/cement interface problem.

Some of the studies have investigated the interface strength and material strength. For instance, Mann et al. (1999, 2001) investigated the bone/cement interface in shear and tension and they concluded that their interface is weak under tensile loads. They also concluded that mixed-mode failure of the bone/cement interface under tensile and shear loads will increase the strength compare to pure tensile loads.

Another area that leads to loosening is osteolysis. As it is mentioned before, osteolysis is an immune response of body to foreign particles. This leads to loss of the implant fixation and finally loosening at the implant area. Osteolysis is a concern because it causes loosening between the implant and bone however, it is not the important and primary problem in the total shoulder arthroplasty.

2.4.3 Inferior Scapula Notching

One of the most common complications after the total shoulder arthroplasty surgery is notching of the inferior scapula by the humeral implant component. (Figure 5)

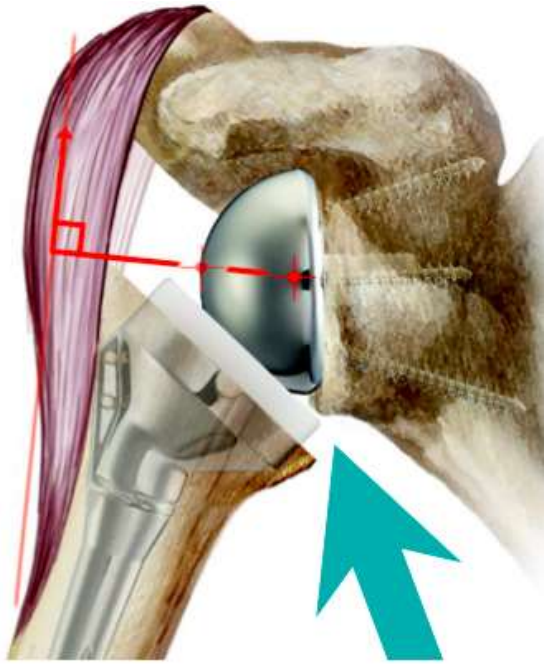

Figure 2.5: Scapular notching (http://shoulderarthritis.blogspot.com/2017/04/scapular-notching-is-it-about-notch-or.html)

This usually happened because of unwanted contact between the proximal portion of the polyethylene of the humeral cup and the bone of the scapula. Sirveaux et al. and Valenti et al. classified the notching phenomena. Werner et al. concluded that this notching appears soon after the implant surgery and it will be stable in most of patients after one year from surgery. They also mentioned that there are still debates over whether the scapula notching causes clinical symptoms.

2.4.4 Dislodgement of the base plate

When the baseplate fixation fails, the glenoid plate and sphere may shift and move which cause the dislodgement. In a study, McFarland et al. showed that screw failure can be seen after the surgery which may cause the base plate failure. (Figure 6)

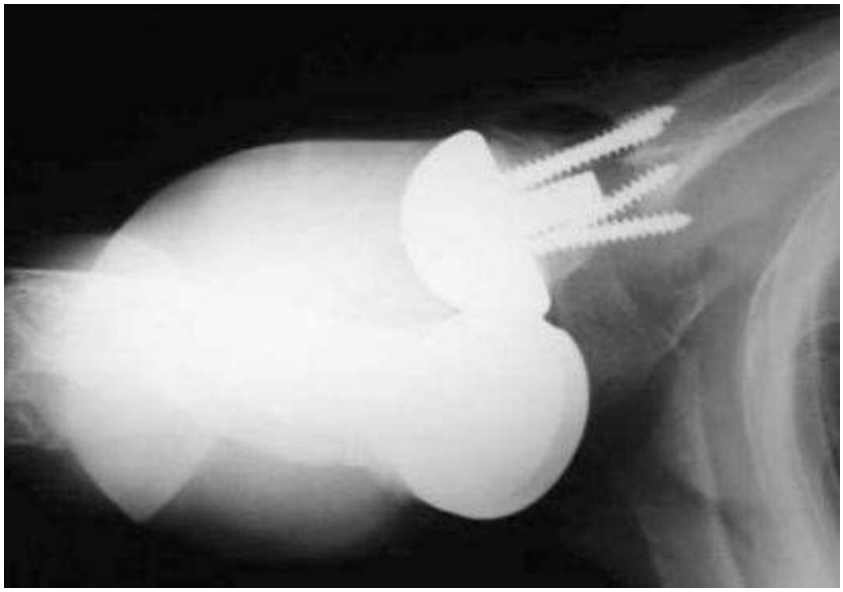

Figure 2.6: base plate dislodgment

2.4.5 Humeral Side Complications

In some studies, such as Sirveaux et al. and Werner et al., the humeral side complications were considered. They concluded that the humeral side complications are uncommon, however, sometimes subsidence of the humeral component happened if it's not well fixed.

2.5 Finite Element Analysis (FEA) of Shoulder Implant

As mentioned in the previous section, arthroplasty surgeries especially total shoulder arthroplasty could have some side effects and problems after the replacement. Some of these problems are inevitable and related to medical situation such as bleeding, infection, blood clots, etc. But some other problems can be prevented such as loosening and dislocation of the joints, failure and fracture from happening by developing the implant design, simulation and finite element analysis before a surgery. Conducting finite element analysis could positively affect the development of the implant design as it shows the maximum stress or displacements in all different components of the implant and also bone components. So, utilizing those results, the implant designers could develop and improve their implant design efficiently. Moreover, a realistic finite element analysis could predict the long term effect of a prosthesis which is helpful for preventing future post-operative problems. Finite element analysis could provide an insight into the different implant components and bone mechanical behavior as design parameters are varied.

In a finite element biomechanical study in 2007, Nazeem et al. designed a model (figure 7) and determined increasing the distance between the glenoid bone and the center of rotation of the

glenosphere increases the base plate dislocation. They conducted a finite element analysis and also an in vitro mechanical testing. Both methods revealed that increasing this distance does not affect base plate dislocation.

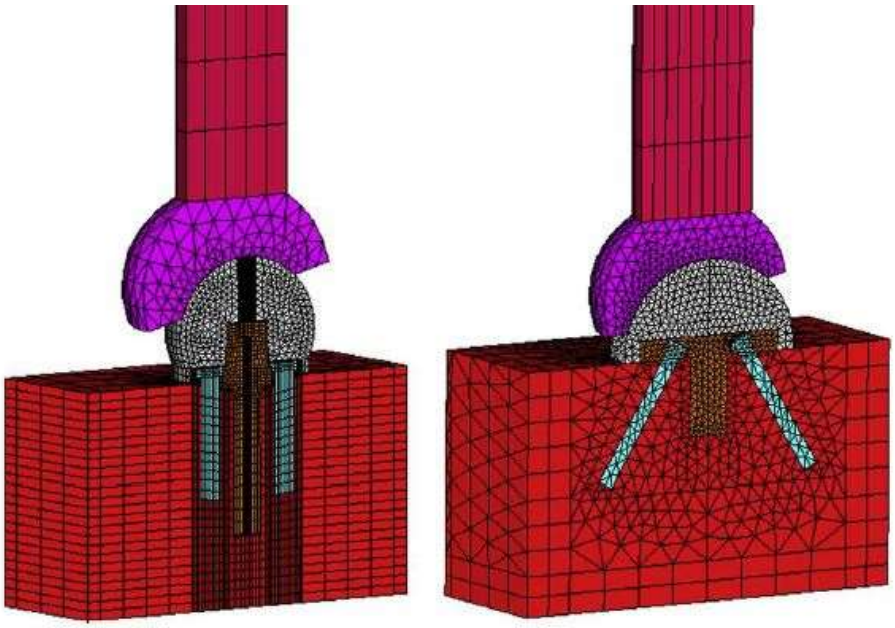

Figure 2.7: Finite element model of the Reverse Shoulder Prosthesis (Nazeem et al., 2007)

In 2009, Hopkins et al. conducted a finite element study on some of the reverse shoulder implant baseplates such as Delta III, Zimmer, Bayley-Walker, RSP-neutral, RSP-reduced and Verso (figure 8). The goal of the study was to investigate the six mentioned implants' abilities to resist interface motions under loading. The results revealed that two out of six existing reverse shoulder implants were reliable and stable.

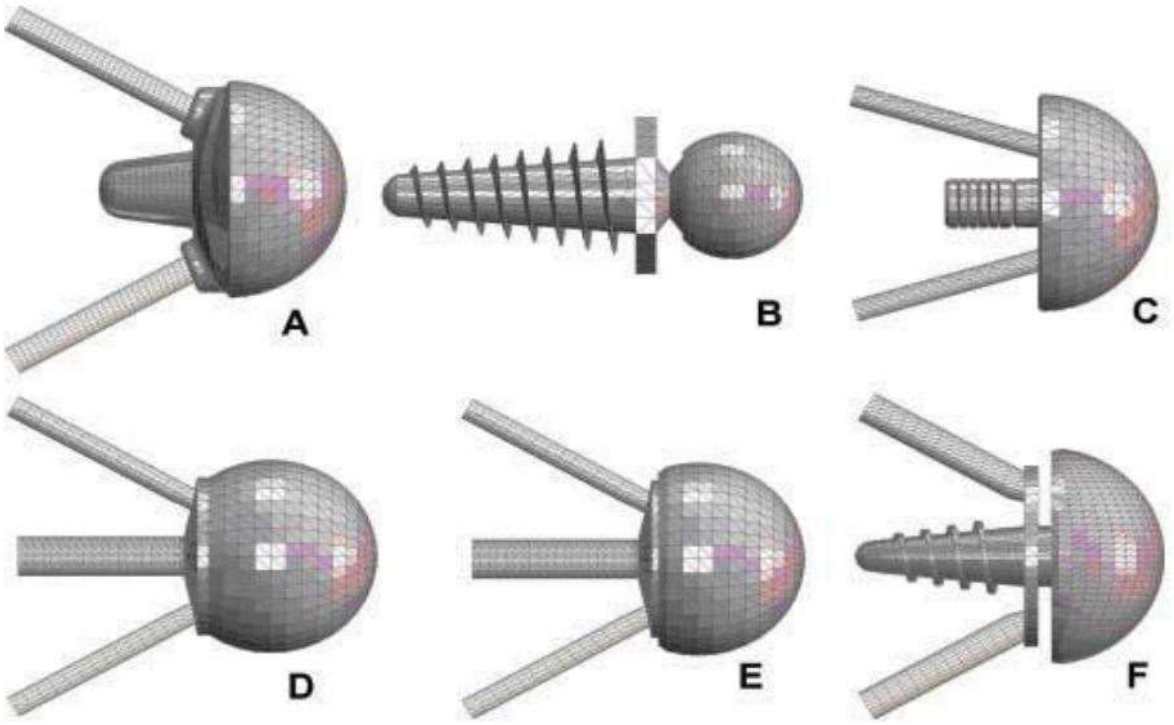

Figure 2.8: finite element models of: (a) Anatomical (Zimmer); (b) Bayley–Walker(Stanmore); (c) Delta III (Depuy); (d) RSPneutral (Encore); (e) RSP-reduced (Encore); (f) Verso (Biomet)

The results showed that when they set the maximum threshold for micro-motion (maximum baseplate micromotion measurement) to 20 µm or 30 µm, it was found that the Zimmer implant is the most stable device between the six tested devices.

Yang et al. in 2013 investigated and determined the effect of various designs of reverse shoulder prosthesis (RSP) on stress variation of its glenoid component using 2-dimensional (2D) finite element analysis (FEA) within ANSYS software (Figure 9). Before this study, several studies have documented that scapular notching could be progressive, clinically significant, and associated with poorer clinical outcomes and also reduced motion and strength. Several solutions such as adoption of gleno-sphere with large diameter, lateral offset, distal offset design, inferiorly tilt of base-plate, and BIO-RSA (bony increased-offset reverse shoulder arthroplasty) have been proposed and documented to avoid notching. Therefore, the purpose of this study was to determine the effect of different designs of RSP on stress variation of its glenoid components to reduce notching and its potential effect on glenoid stability. They stablished a 2D finite element reverse shoulder model (FERSM) on 2D human shoulder with implementation of RSP. They consider all the mechanical properties of the model components and applied it to the simulation. Also, the distributions of von

mises stress of glenoid component were investigated in this article. For the verification of the study the authors have assigned similar parameters as mentioned by Harmon et al into their 2D FERSM. As a result, they have found a similar trend on the interface micro motion plotted with various amount of lateral offset between Harman et al experiment and the present results under the same testing condition. Furthermore, the study compares the effect of screw patterns on stress distribution. They found that divergent pattern exhibits less micro motion than the convergent pattern. As scapular notching is one of the common postoperative problem, investigation of various designs that potentially prevent notching are important for the long-term survival of prosthesis.

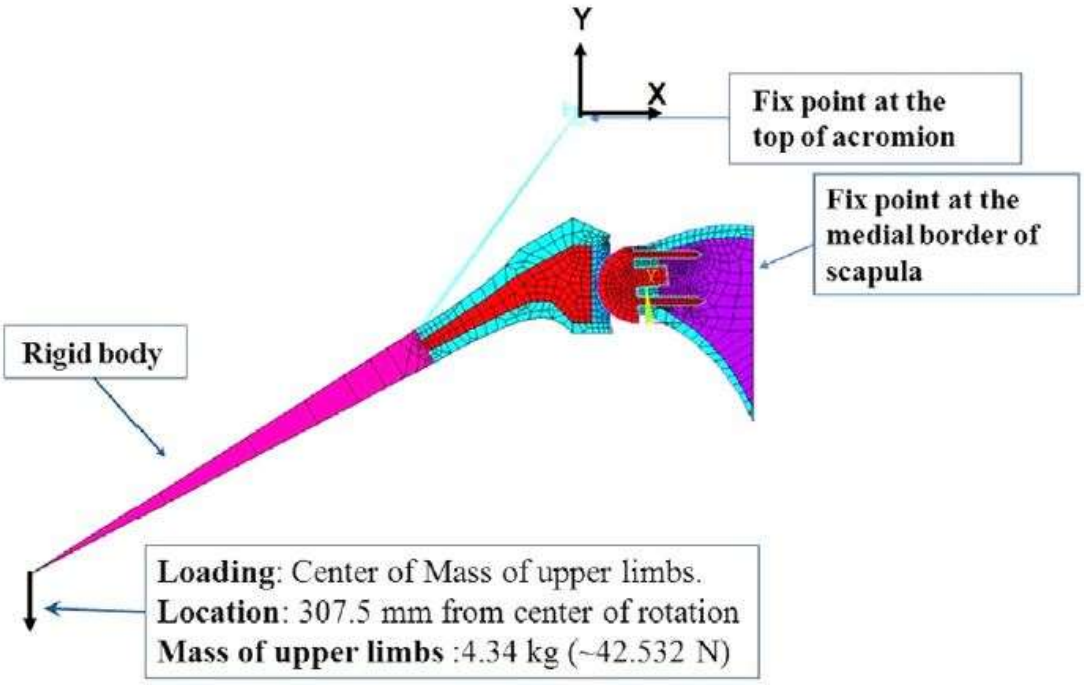

Figure 2.9: 2D finite element reverse shoulder model and its boundary (Yang et al. 2013)

Thereby, considering their 2D FERSM, the paper demonstrated that the solutions, potentially reducing scapular notching, will increase stress concentration over baseplate and its fixation screws of the reverse shoulder prostheses. Regarding the von mises stress distribution of RSP in full model, base plate and screws they mentioned that the maximum von mises stress of full model occurred at the distal interface of the implant and humerus. With respect to the screws, the maximum von mises stress of inferior screw was larger than that of superior screw. Additionally, there is stress concentration located at the base of inferior screw, which may correlate with the occurrence of radiolucent zone around the inferior screw.

In 2016, Dennard et al. evaluated the impact of glenoid-sided lateralization in RSA (Reverse Total Shoulder Arthroplasty) using a FEA model, and compare bony and prosthetic lateralization. Before this study several studies have documented that several design modifications to the Grammont design have been proposed to decrease scapular notching such as a more vertical humeral neck-shaft angle and lateral offset. Several studies have been proposed and documented that the latter may be accomplished by either prosthetic lateralization of the glenosphere and/or baseplate component, or via bony increased offset (BIO-RSA). Therefore, the purpose of this study was to provide a finite element model in order to assess glenoid-sided lateralization in reverse shoulder arthroplasty. They stablished a 3D finite element reverse shoulder model (FERSM) on 3D human shoulder with implementation of RSP. Four different lateralization configuration has been done; lateralization via bone graft, metallic lateralization via the baseplate. metallic lateralization via the glenosphere (figure 10).

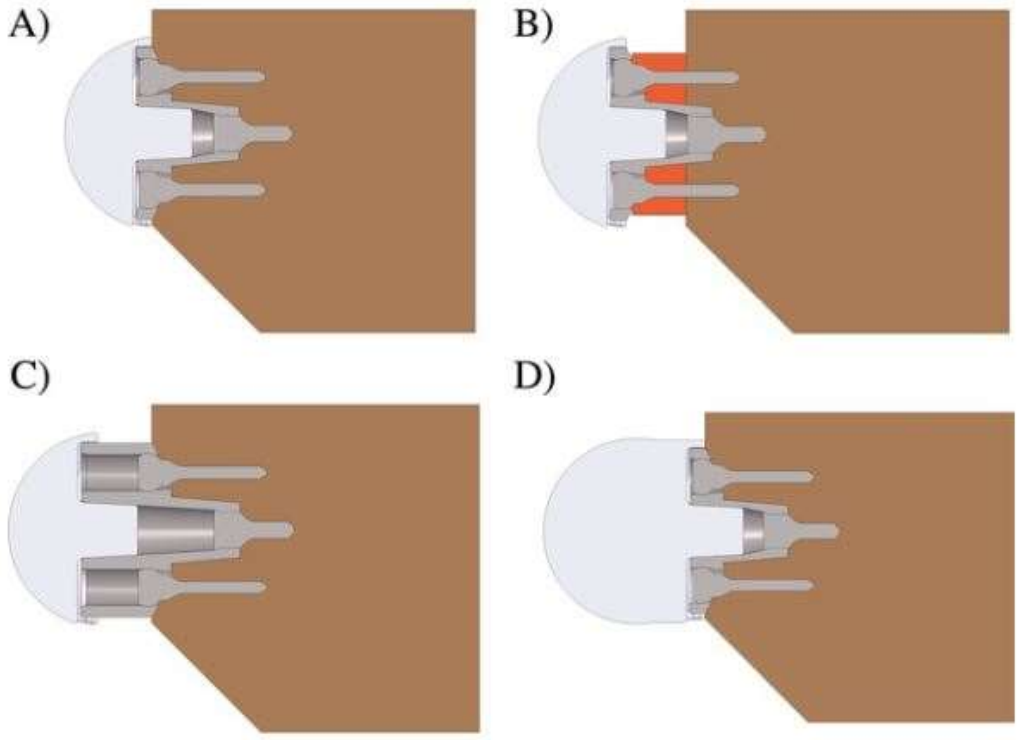

Figure 2.10: Lateralization models. (A) No lateralization, (B) Lateralization via bone graft, (C) Metallic lateralization via the baseplate, (D) Metallic lateralization via the glenosphere. (Dennard et al. 2016)

They consider all the mechanical properties of the model components and applied it to the simulation. Also, they have done stress analysis in different components in this article. As a result, they have found that baseplate stress and displacement in an FEA model is lower with a smaller

glenosphere, inferior tilt, and divergent screws. Bony lateralization increases stress and displacement to a greater degree than prosthetic lateralization. Furthermore, it appears that at least 10 mm of prosthetic lateralization is mechanically acceptable during RSA, but only 5 mm of bony lateralization is advised.

2.6 Conclusion

Reverse shoulder arthroplasty is a good option for patients who suffer from rotator cuff muscle tearing and a cuff-deficient shoulder. However, there are some contraindications such as axillary nerve deficit such that deltoid function is inadequate, inadequate glenoid bone stock to secure the glenoid component, active infection, and also for young patients. Though, there are debates about the indications and contraindications such as what age of patient count as too young to undergo this surgery. However, some of the literatures demonstrated some improvements in pain and ROM (range of motion) after the surgery which make the reverse total shoulder arthroplasty an increasingly popular selected option for patients who have suffered from rotator cuff muscle tearing and tendonitis.

For the evolution of the reverse total shoulder arthroplasty designs, researchers need to consider many variables of constrained shoulder arthroplasty. The review showed the improvement of reverse shoulder arthroplasty specially in the current issues relevant to reverse shoulder arthroplasty, the biomechanical variations in the evolution of this arthroplasty, and the evolution of reverse shoulder arthroplasty designs.

Nowadays, the reverse total shoulder arthroplasty implant design is different in certain design details, though, the base design is based on the Grammont's principals. The problems and complications of the reverse arthroplasty such as infection, scapular notching, instability, acromial insufficiency, and glenoid component failure have been described extensively in the current literature.

Without a shadow of a doubt, the modern reverse total shoulder arthroplasty design improvement is an interesting and crucial aspect of orthopaedic surgery. As reverse total shoulder arthroplasty area is an advance field of research and different systems have been developed so far, there are some controversies on the center of rotation medialization, with some proposing a more lateral

offset. Some of the researchers suggest that the more lateral center of rotation causes a lower rate of scapular notching and consequently less impingement in glenoid and scapula area. On the other hand, the proponents of the more center of rotation medialization propose that with considering a proper position of the more medial glenoid component, the notching might also be minimized. Therefore, additional high-quality research is needed to overcome these issues and controversies.

Chapter 3. Methodology and Data Collection

3.1 Introduction

3.1.1 Body Planes

The range of movement of the shoulder joint (abduction, adduction, flexion, and extension) were discussed in chapter one. As the different body planes play a crucial role in utilizing ABAQUS and Mimics software, it is worth reviewing the different body planes for the desired analysis. Figure 1 illustrates the different body planes.

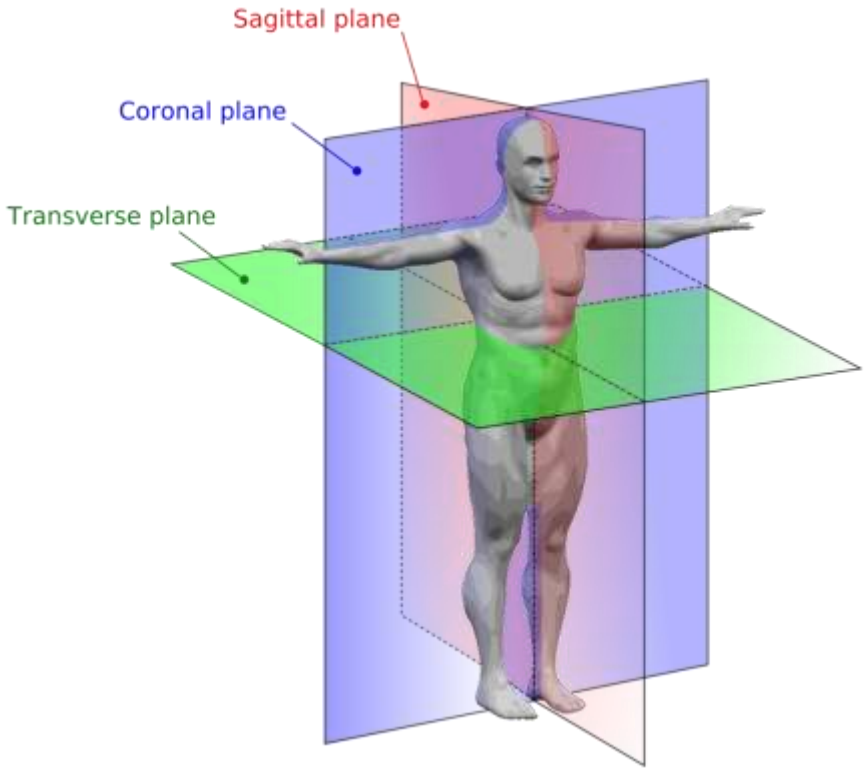

Figure 3.1: Body planes ***(https://courses.lumenlearning.com/austincc-ap1/chapter/practice-anatomical-location/)***

3.2 Methodology

Five software were utilized in this study: Mimics, SolidWorks, 3-matics, ABAQUS, and SPSS.

Using Mimics, the 3-D bone geometries were developed from CT-scan images and also the heterogeneous scapula bone mechanical properties were assigned. The set of CT images was pre-processed within Mimics to remove artifacts and also to further enhance the image quality.

The next software is SolidWorks which was utilized to design the implant components' geometry. This software is commonly utilized for mechanical components design purposes. The compression screws and base-plate was designed within SolidWorks, then the whole components including the imported scapula bone model from Mimics, were assembled.

ABAQUS software is a commonly used software for simulation of the manufacturing systems and material behaviors. Therefore, the loads distribution across the implant components such as screws and also the relative micro motions between the bone and implant were analyzed using ABAQUS.

3-matics software was used for applying the mesh configuration and lining up the meshed scapula bone with the primary scapula bone that has been created from CT-scan images. This is helpful for the procedure of assigning the bone mechanical properties within Mimics.

In the following sections, the step-by-step procedure of utilizing the Mimics, SolidWorks, 3-matic and ABAQUS, and SPSS software which are the main software for conducting this project will be introduced and described.

3.3 Mechanical Testing Experiment

The mechanical tests were carried out at Western University, Ontario, Canada. To simulate the micromotion of the glenoid's baseplate under mechanical loading a series of tests were set up. A custom fixture was designed and manufactured in the workshop for fixing the scapula. Figure 2 illustrates the designed fixture used to lock the glenoid movement.

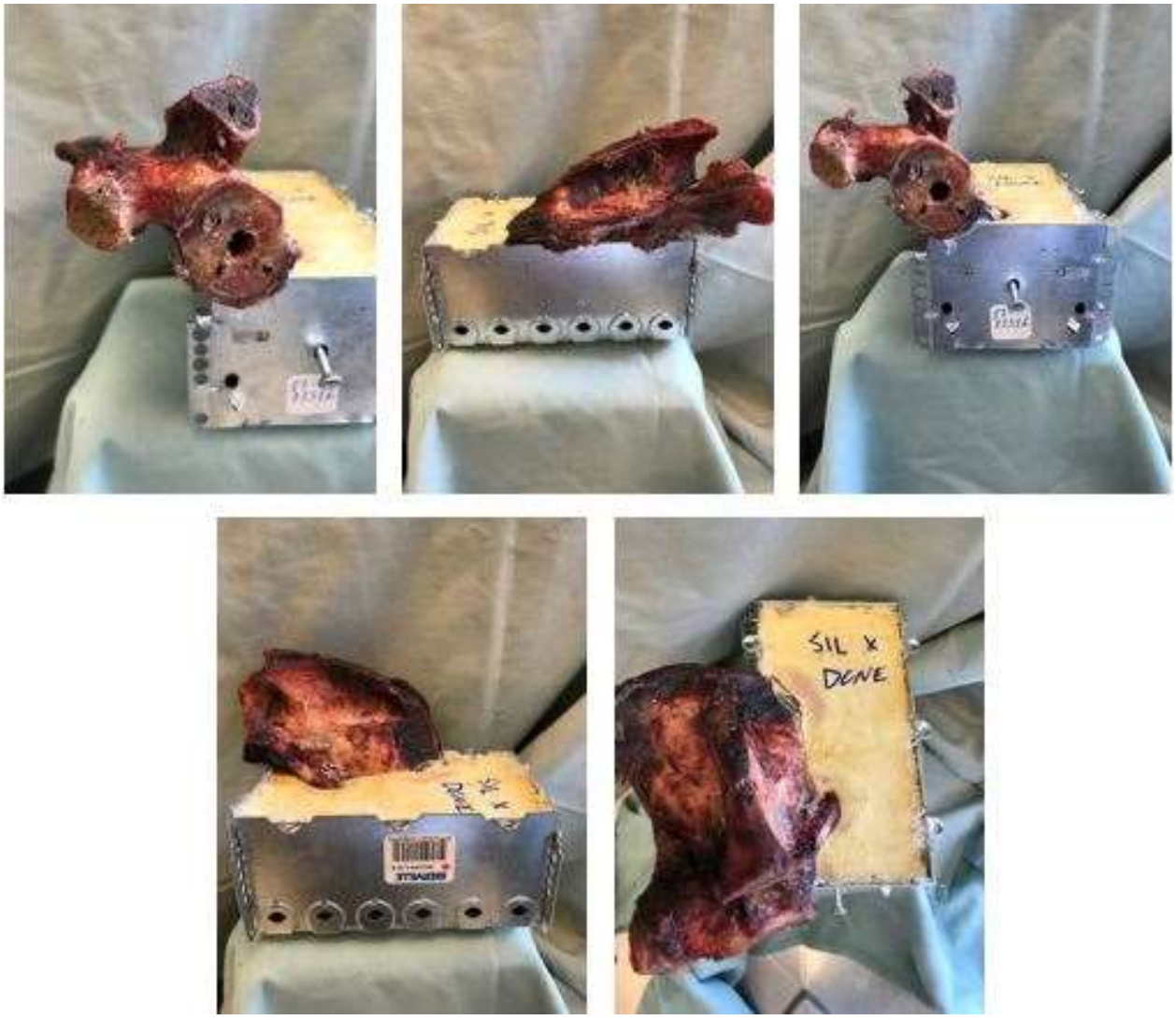

Figure 3.2: designed fixture used to lock the glenoid movement

3.3.1 Baseplate

The base plate had two divergent screw configurations in superior and inferior sides placed at a divergent angle of 15 degrees and two parallel screws in anterior and posterior sides.

There were six different scapula specimen including three different cadavers' scapula with right and left scapula. There were two screw configurations used in this experiment; one of the configurations was superior-inferior locking screw and the other configuration was anterior-posterior locking screws. However, in all of the configurations the superior and inferior sides were divergent screws and two parallel screws for anterior and posterior sides.

3.3.2 Loading Protocol

Micromotion for this experiment was defined as the displacement between the resting LVDT position before and after load was applied.

Load was applied at 6 different eccentricities (±2 [cm], ±3 [cm], ±4 [cm]) where positive represents eccentric positions superior of the superior edge of the glenoid baseplate, and negative represents eccentric positions inferior of the inferior edge of the glenoid baseplate. Superior-Inferior as defined by the 12 to 6 o'clock axis of the glenoid fossa. Positions were tested in the order +2, +3, -2, -3, -4, +4 [cm].

Load was applied statically for 30 seconds then load was removed for 30 seconds starting at 0N and stepping up by 50N until 300N was reached. This protocol was repeated at each position in the order indicated above. These loads were applied perpendicular to the plane of the glenoid baseplate. The eccentric loads were applied on a rigid body that was attached to the glenoid baseplate. This way, the applied load was carried to and distributed on the base plate.

The data used for comparison to the finite element simulations represent the displacement at the time while the load was applied.

Micromotion data, pictures of post operation for the left and right scapula, and CT-scans were provided from the experiment for conducting the simulations.

The micro motions were acquired using Linear Variable Differential Transformers (LVDT); LVDTs are used to measure displacement. LVDTs operate on the principle of a transformer. A LVDT consists of a coil assembly and a core. The coil assembly is typically mounted to a stationary form, while the core is secured to the object whose position is being measured. The coil assembly consists of three coils of wire wound on the hollow form. A core of permeable material can slide freely through the center of the form. The inner coil is the primary, which is excited by an AC source as shown. Magnetic flux produced by the primary is coupled to the two secondary coils, inducing an AC voltage in each coil.

Regarding the three degrees of freedom (DOF) baseplate motion definition and to create a coordinate system, the LVDTs were used. Using the known rigid position relationship between

the baseplate and LVDTs, micromotions, or baseplate displacements, were computed at the superior and inferior edges of the implant by transforming the measured LVDT data to the edge of the baseplate. [S. Abdic et al.]

The micro motions were extracted by considering the baseplate edge. When the loads were applied on superior eccentricities, the micro motions were acquired by measuring the micro motion of the inferior baseplate edge. When the loads were applied on inferior eccentricities, the micro motions were acquired by measuring the micro motion of the superior baseplate edge.

3.4 Simulation

3.4.1 Introduction

This section will provide the information regarding the simulation of the experimental study. The procedure of simulating the experiment will be discussed step by step.

Some assumptions were considered for this study. At the compression screw-baseplate interaction there are rotational degree of freedom (DOF) which are only restricted by friction. Owing to the fact that the compression load is high, it was assumed that the friction resistance is adequate to significantly limit screw-baseplate rotations. Therefore, within the model, these rotational degree of freedom were ignored and the screws were modeled by integrating the compression screw heads within the baseplate. Another assumption relates to the loads applied. In the experiment, the forces were applied on a rigid body attached to the baseplate at known eccentricities; however, in the simulation experimental loads were replicated using the couple feature in Abaqus software, the equivalent forces and moments were applied at the baseplate center, which add a bit of simplicity to the simulation as the coupling feature helps to constrain one surface movement to one node.

Regarding the screw geometry; according to Inzana et al., considering the screw threads in the design does not affect the finite element results and just increases the computational cost and simulation time significantly. Therefore, in this study the screw threads were not modeled. Both the locking and compression screws were considered as cylinders. In SolidWorks, a gap was considered in the compression screws design in order to apply the preload properties in ABAQUS using the Bushing Connector feature. The details will be elaborated in the following sections.

In order to conduct the simulation, four software were used. At the first step for each specimen the 3D scapula bone geometries were extracted using Mimics.

SolidWorks was used for designing the baseplate with features same as the baseplate was used for the experiment and then reaming the scapula bone and assembling the bone and baseplate the way it was done at the experiment.

Then the model was imported to the 3matic software for applying the appropriate mesh configuration and aligning the current model with the basic model generated from CT-scan images via Mimics. The reason of doing that was to prepare the bone model for applying the heterogeneous mechanical properties on the scapula bone using Mimics at the next step.

The extracted models from Mimics were then imported to the Abaqus software for conducting finite element analysis and defining the interactions, applying loads and moment, compression screws preload, and boundary conditions similar to the experiment.

Finally, the results were acquired from Abaqus to analyze the micromotion of the baseplate under the defined load, moment and conditions.

3.4.2 Methodology

The methodology of this simulation is illustrated in the following flowchart. (figure 3)

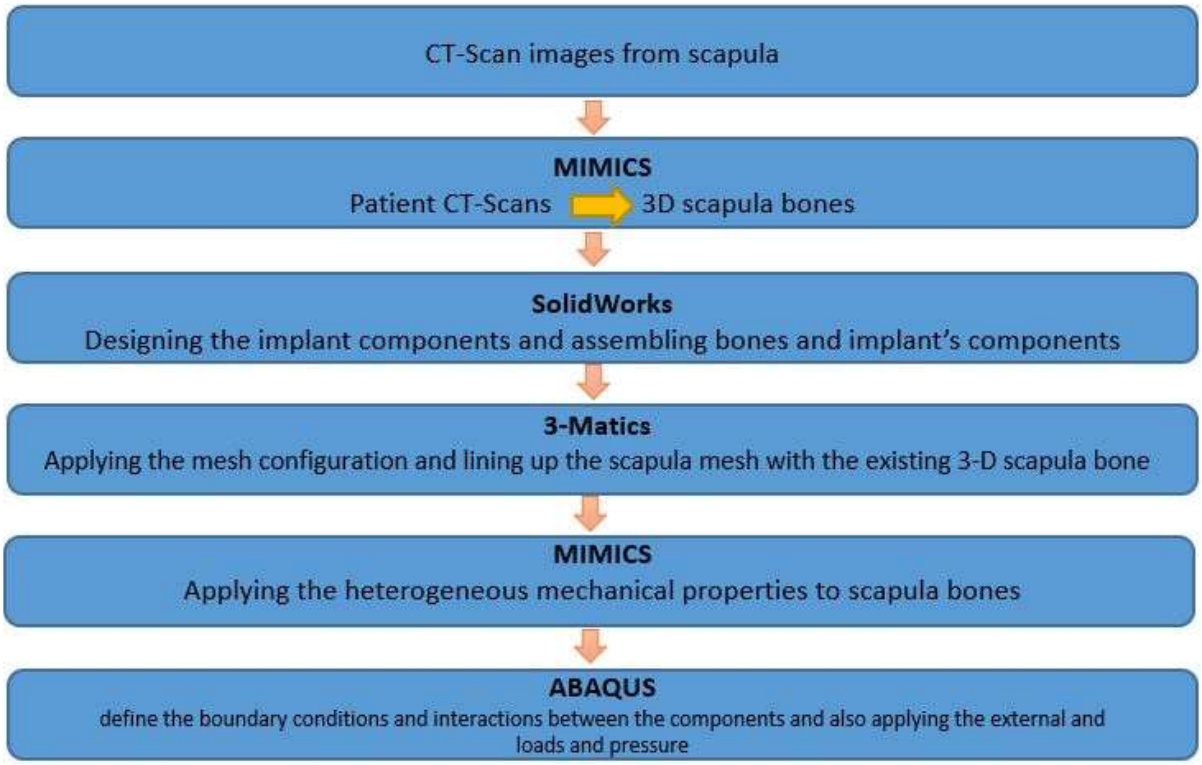

Figure 3.3: General simulation flowchart

3.4.2.1 MIMICS Software

Mimics read CT- scan and MRI (Magnetic resonance imaging) data in the DICOM format interactively. Regarding the manipulating the data to select and separate bone, skin, and soft tissue, this software has provided segmentation and editing tools. The area of interest could be visualized in three-dimensional when the bone is separated from the other areas. Once the procedure is done, the .STL file could be exported from this software.

Mimics has a number of different modules. Figure 4 illustrates the overall procedure of the modules of Mimics and the imported and exported files.

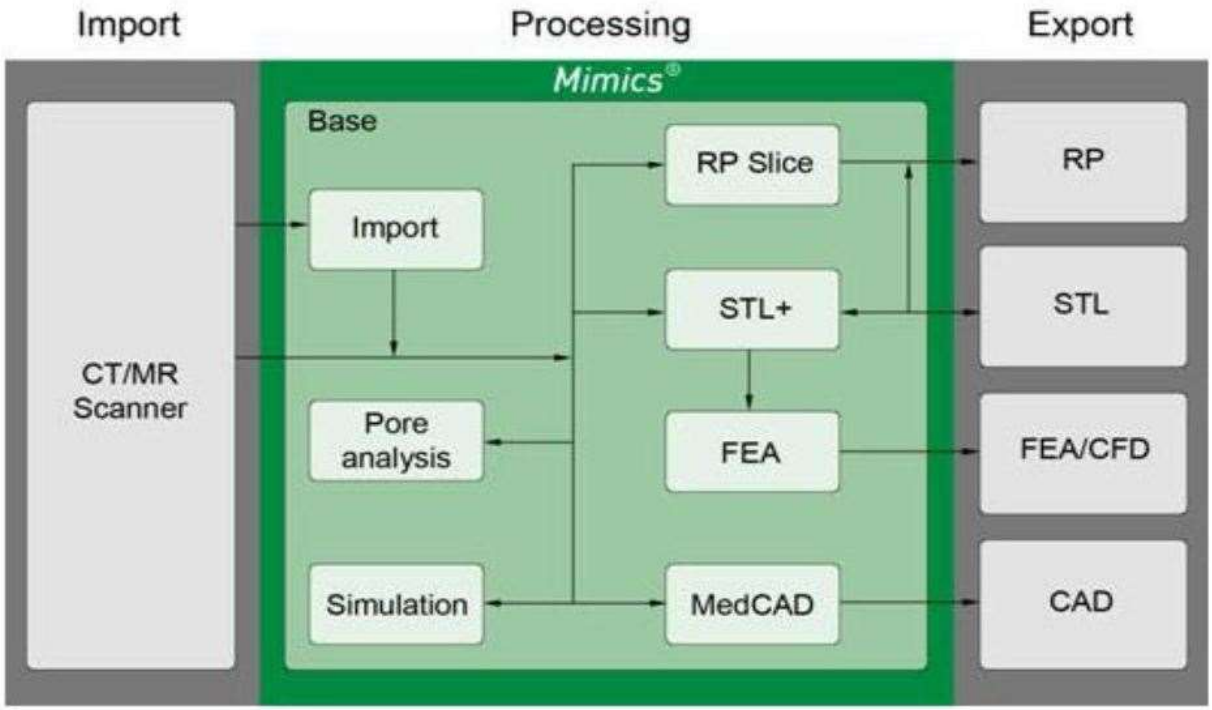

Figure 3.4: Mimics modules (Mimics tutorial)

Using Mimics, the researcher would be able to assign meshes to the generated 3-D model. The volumetric mesh and the assigned mechanical properties could be exported from Mimics and then imported to some software such as ABAQUS, ANSYS, and Patran Neutral for the finite element analysis purposes on the defined meshes.

Therefore, the goal is to generate a representative 3D surface mesh of the scapula bone via Mimics which could be exported to SolidWorks and then to ABAQUS for finite element analysis.

3.4.2.2 Importing CT-scan Images

The automatic import wizard was utilized to import the CT-scan images. In the GUI select File and then import images to start the import wizard. The resulting mask was segmented into one specifically for the scapula, and this mask was converted into a part. In the next step the scapula model needs to be smoothed and wrapped and afterwards exported as an .STL file and then imported into SolidWorks as a solid body.

It is good to be mentioned that, T and B stand for top and bottom, A and P stand for anterior and posterior, L and R stand for left and right. Mimics could be processed after importing CT-scan

images to increase the images quality and creating the three-dimensional model precisely. There are some tools available in Mimics to conducting the image processing such as thresholding and region growing.

The exported images from CT-scan apparatus were in the DICOM format. Some file formats, for instance DICOM, are known to Mimics and could be imported automatically. The high image resolution associated with the reduced distance between slices assures an acceptable geometrical definition and surface topography of the primary three-dimensional models afterwards when the density segmentation operations will be performed. (figure 5)

The image slices in the DICOM format were selected and automatically imported to Mimics. The pixel size was automatically computed accounting the present image resolution. Actually, the parameters that could positively affect the dimensional coherency of the model during the segmentation process is the pixel size and the resolution of the image. The image slices were then stacked and converted to be displayed in axial, coronal, and sagittal plane views. The orientation of each view was defined before continuing.

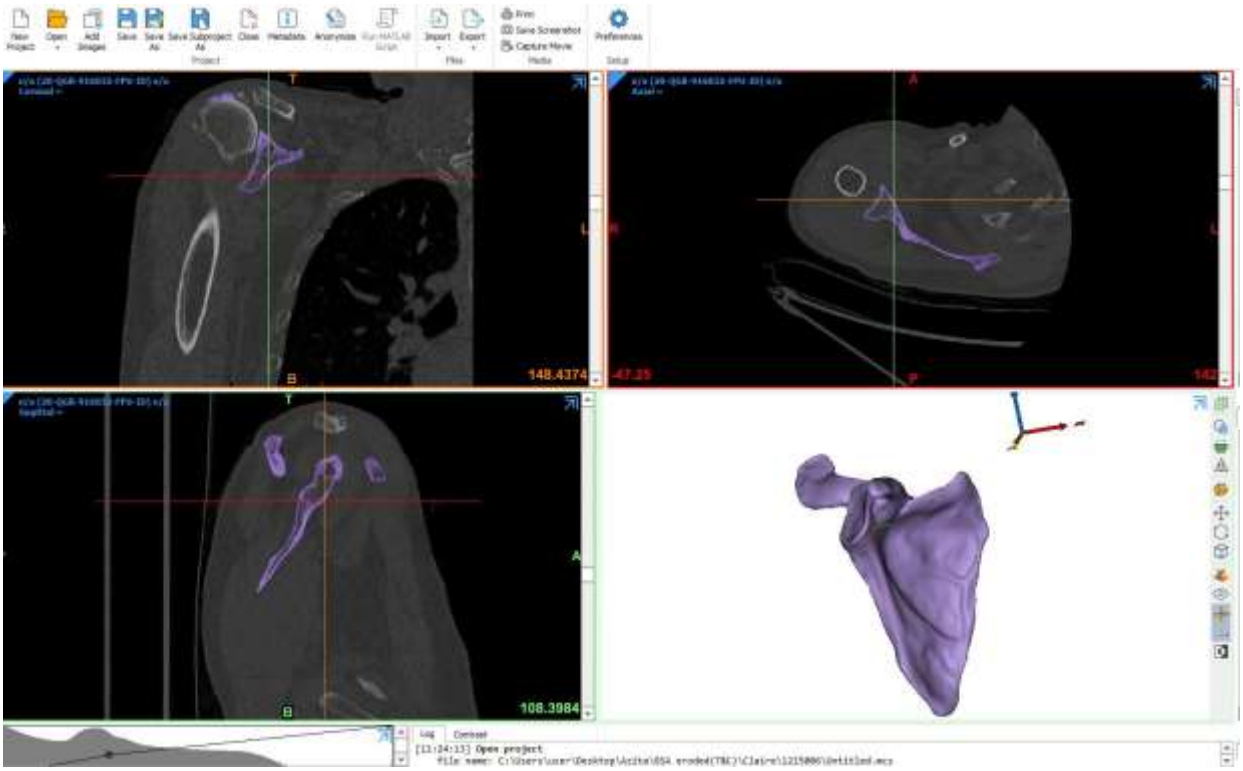

Figure 3.5: Axial (top right), sagittal (bottom left) and coronal (top left) views of the scapula

3.4.2.3 Thresholding

The first action performed to create the segmentation mask is thresholding. The region of interest boundaries has the lower and upper threshold value in that range. The pixels in that range with a grey value will be highlighted in the mask. The threshold has been done using the toolbar in the GUI for the imported CT-scan images. Defining threshold would help the software to specify the tissue type and it still could be altered. The threshold value could be changed using the sliders in the thresholding toolbar.

As it is illustrated in Figure 5, the segmentation area changes according to the threshold value changes. The user could set the minimum and maximum value for the threshold. In the thresholding dialogue box, adjust the slider to define the threshold. Different type of materials on the CT-scan image was highlighted by a brighter color as the slider is adjusted. The slider should be adjusted only to the point that the cortical bone is most brightly highlighted. For instance, as it is illustrated in the figure 6, the minimum and maximum threshold is defined as 226 HU and 3071 HU respectively. The thresholding tool separates the created segmentation into different objects and also removes the floating pixels.

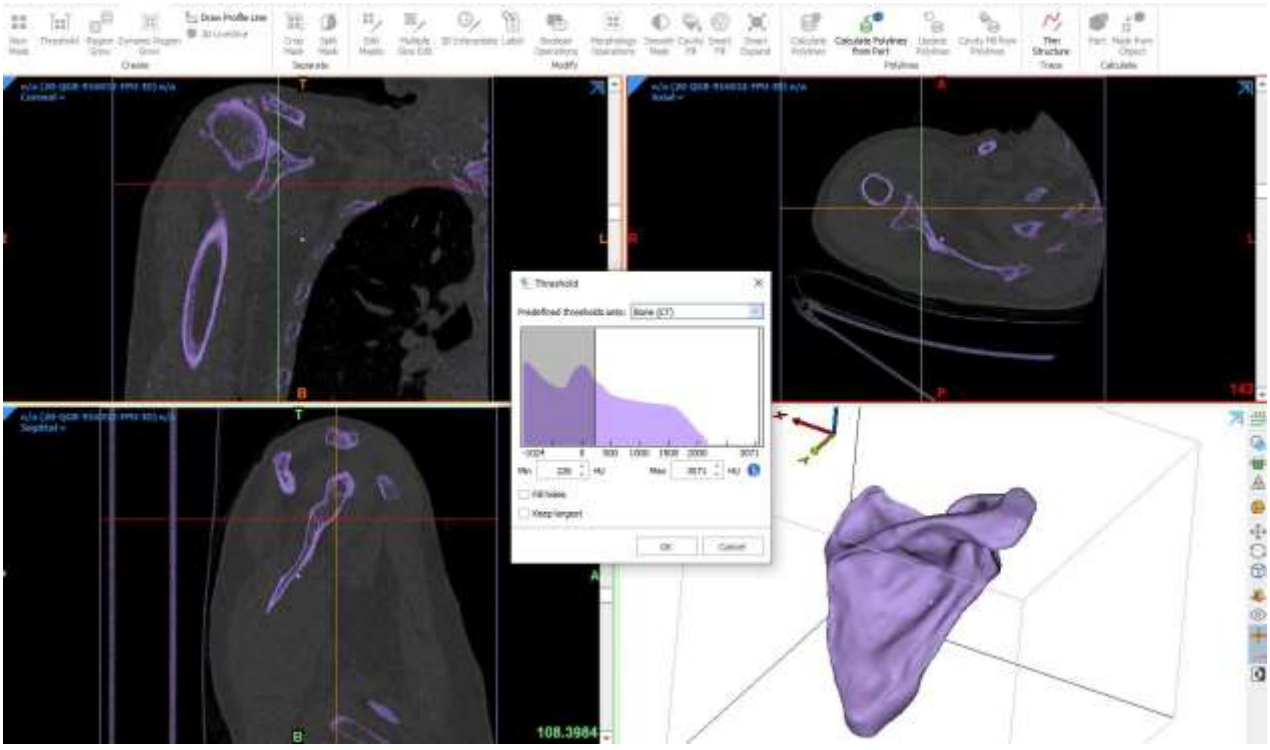

Figure 3.6: Dialogue box for setting the thresholding

As it is shown on the figure 7, the purple mask has been assigned to the scapula.

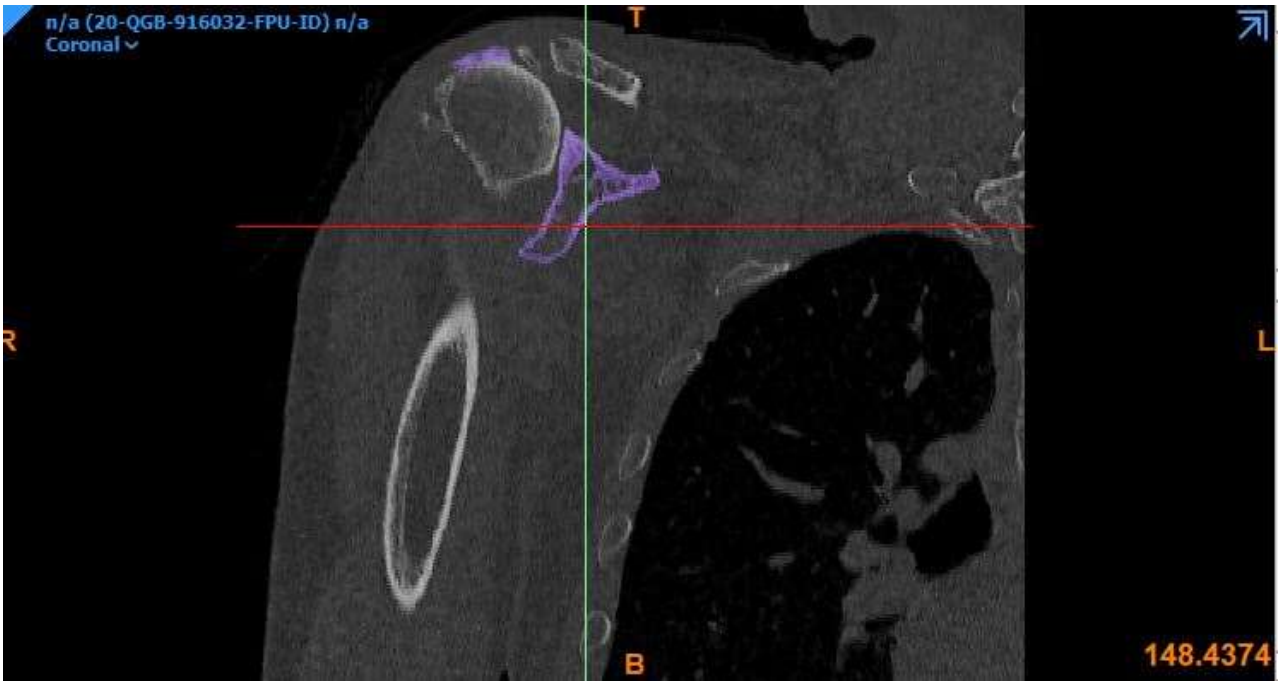

Figure 3.7: Purple mask assigned to the scapula

3.4.2.4 Region Growing

By clicking on the region growing icon, a dialogue box that contain the instruction to select a boundary will appear. The region growing splits the segmentation into different entities. This way enables the user to generate individual geometrical components and thereafter three dimensional models. Also, artefacts and redundant pixels were manually eliminated. The cavity filling operation was manually performed using the multiple slice editors to eliminate existing vacancies in the density masks. (figure 8)

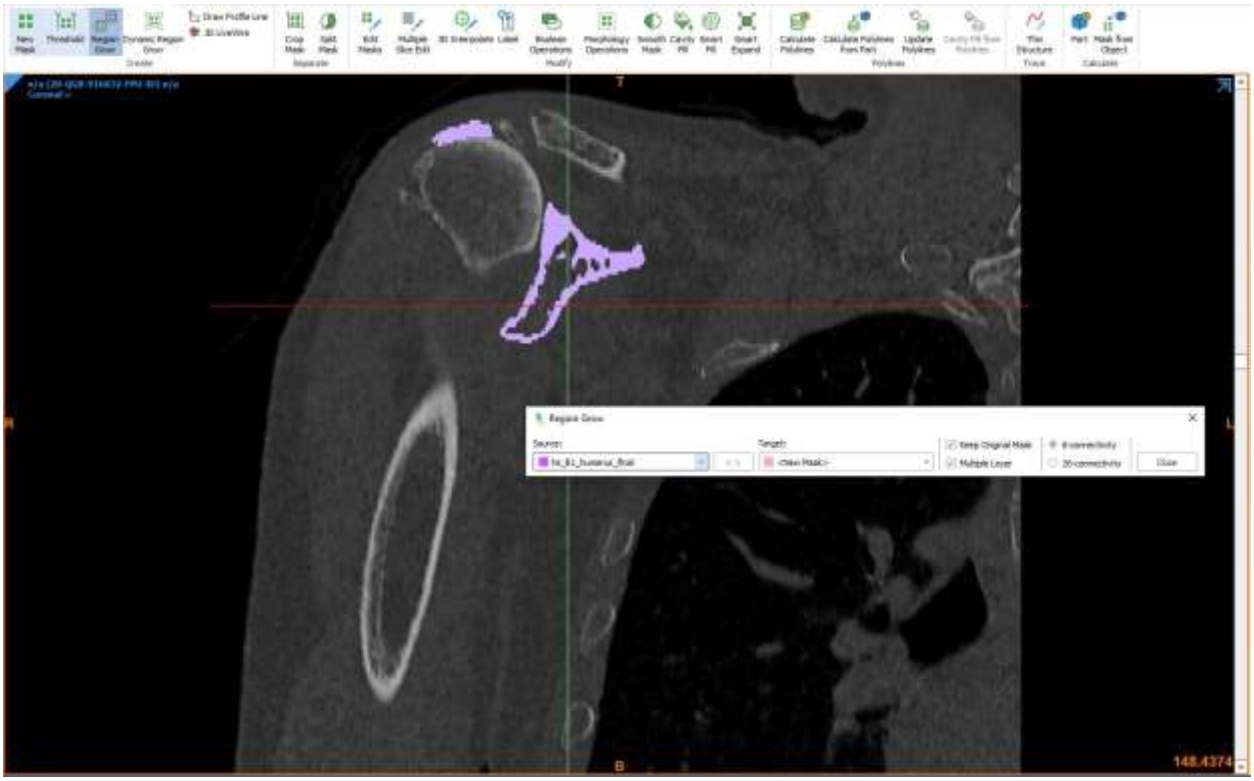

Figure 3.8: Mimics, icon for region growing function

3.4.2.5 3D Model Creation

Regarding the scapula bone, for acquiring three-dimensional geometry the computation was carried out on the density masks generated for this bone. Afterwards, the 3-D model were wrapped and smoothed using the smooth factor to acquire a proper surface topography. Calculating three-dimensional scapula bone via Mimics is the closest representation of the real bone geometry. Afterwards, the wrapping and smoothing of the surface will omit the extra parts in the model.

3.4.2.6 Exporting the bone model

The last step in Mimics is exporting the three-dimensional scapula bone geometry. As illustrated in figure 9, using GUI in the export section, the binary STL has been chosen and then in the part section one can choose a certain model and add it to object to convert section.

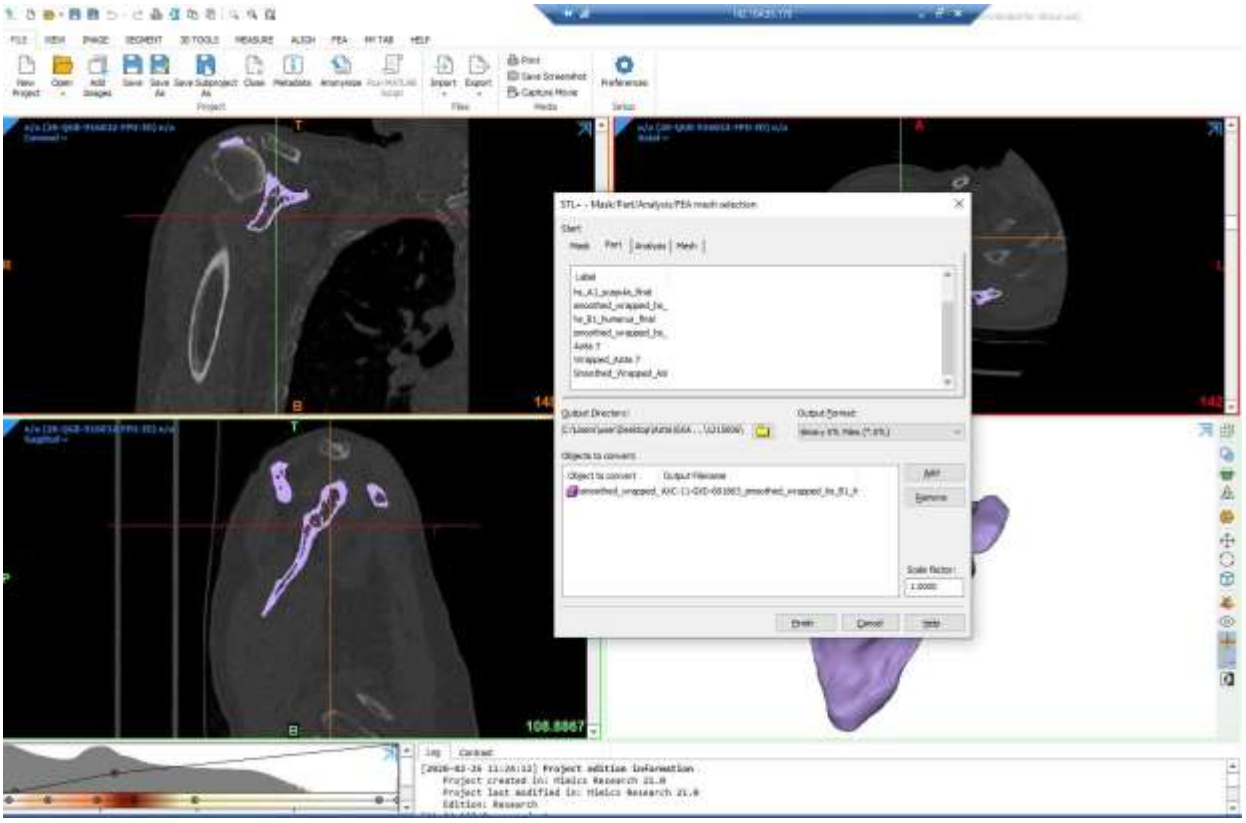

Figure 3.9: Export steps of STL files

The experiment was done on three different cadavers with totally six scapula bones. CT-scan images from the cadavers were provided. Using the CT-scan images, similar to the procedure provided in chapter three, the three-dimensional scapula bone geometry for the six specimen were extracted as .STL files. Figure 10 illustrates one of the 3-D scapula bone models.

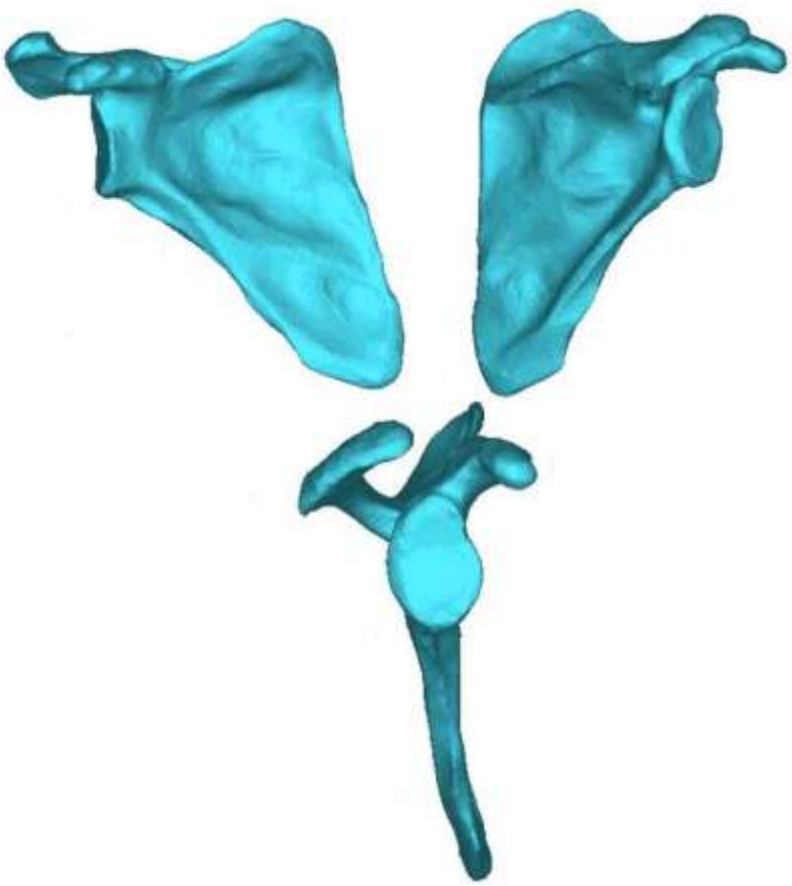

Figure 3.10: 3-D scapula bone model in three different views in mimics

Also, after using 3matic, for applying the heterogeneous material properties on the scapula bone, as the CT-scans contained CT calibration phantom, the density-hounsfield unit (HU) relations for each model were extracted using the sphere feature within mimics and some relations in literature. (Werner et al., 2014, Andrew et al. 2020, Jonathan K et al., 2019).

CT calibration phantom is composed of a plastic base material containing five rods of reference material embedded in the plastic base. The base material is not used as a reference material. The Reference materials contain known and varying amounts of low and high atomic number materials. Figure 3.11 shows a CT calibration phantom with five embedded rods.

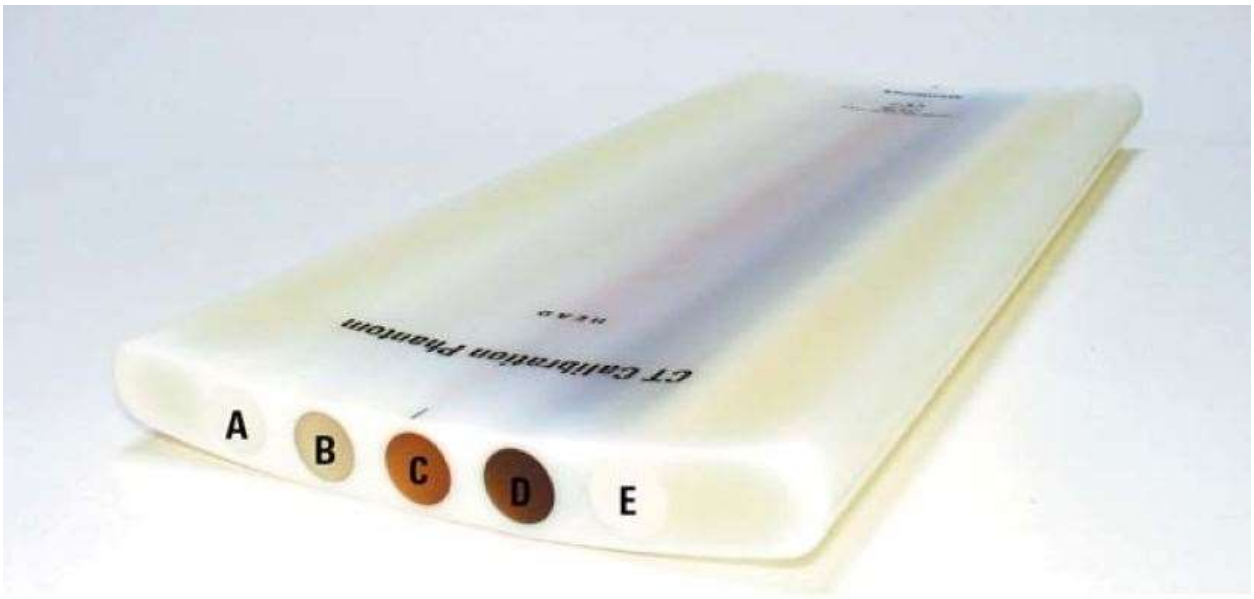

Figure 3.11: CT Calibration Phantom

The CT calibration phantom contains tubes of reference material which are 0.75 inches (19 mm) in diameter approximately. This provides a reference area of approximately 285 mm^2. A circular region of interest (ROI) of approximately 50% of this area, which is 150 mm^2, provides sufficient precision for the CT number measurement while eliminating the need for highly precise positioning of the ROI within the reference area. However, care should be taken, not to place the ROI too close to the edge of the reference area in order to minimize partial volume errors in the CT number measurements. Figure 12 demonstrates how to place the region of the interest.

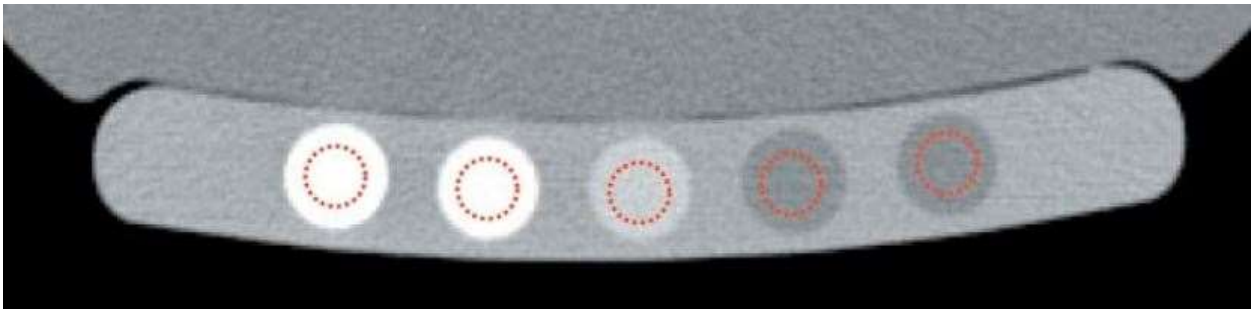

Figure 3.12: Region of interest for each rod

Figure 13 and 14 illustrates the use of ellipse feature to measure average hounsfield unit of each rod for the CT-scans of cadavers used in the experimental study within Mimics and the hounsfield-density measurements extracted from the equations in literature respectively.

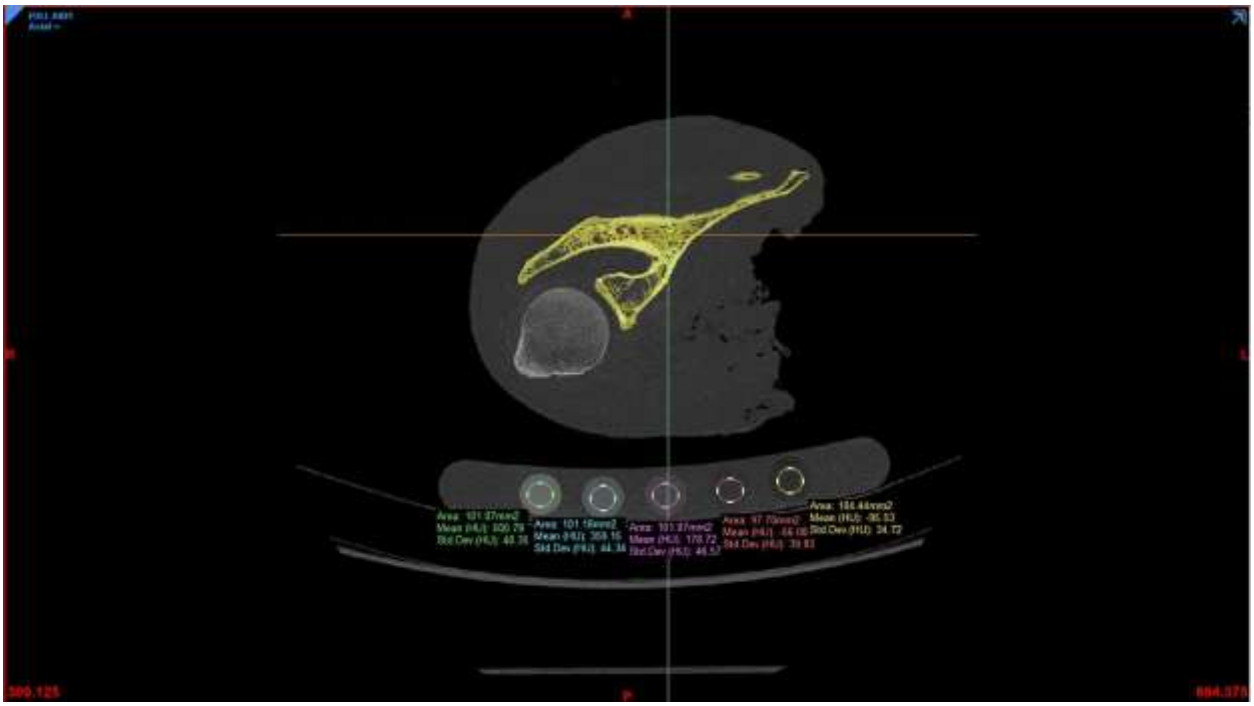

Figure 3.13: Using sphere feature to measure average Hounsfield Unit of each rod

Figure 3.14: The minimum and maximum HU and equivalent density were imported within mimics

The scapula bone has different mechanical and material properties in its different geometry. So, material properties in the scapula are heterogeneous and therefore, density and elastic modulus have significant spatial variance [Daalder et al. 2018]. In order to apply these heterogeneous properties, density values were assigned to each node of the scapular volume mesh based on the

intensity of the CT scans and the elastic modulus was calculated using the following correlation [Knowles et al. 2019]:

$$E = 32790*\rho^{2.307}$$

Furthermore, for applying the heterogeneous material properties on the scapula bone, two material types were considered. First, a single density of $\rho = 0.05 g/cm^3$ accounted for all hounsfield unit values below zero in the CT-scan; for the finite element analysis, these negative values would cause serious errors. 100 material types between certain density which was extracted from the excel file were considered for the second type. (Gupta et. Al)

3.4.2.7 SolidWorks

Using SolidWorks, baseplates were modelled. Instead of a baseplate and four separate screws, a monoblock baseplate-screw components was used as these two models are equivalent and produce same results (Studders et al. 2019). According to the experiment, two screw configuration were considered in the models; APLS (Divergent compression screws located inferior and superior and two parallel locking screws located anterior and posterior), and SILS (two parallel compression screws located anteriorly and posteriorly and two divergent locking screws located superiorly and inferiorly). Similar to the experiment, the screws were designed such that they were tilted from the central baseplate peg at an angle of fifteen degrees. Figure 15 and 16 illustrates the APLS and SILS baseplates respectively.

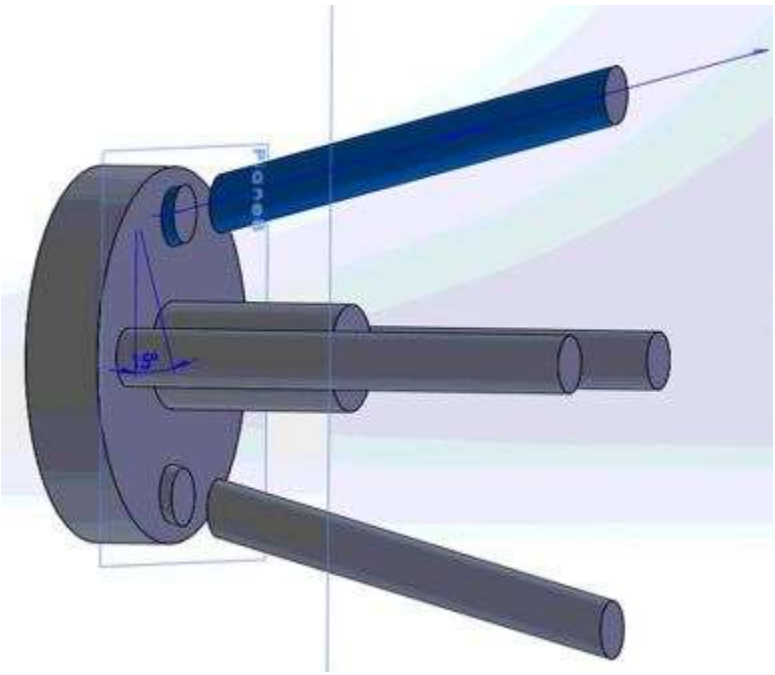

Figure 3.15: Designed baseplate with anterior-posterior locking screw configuration

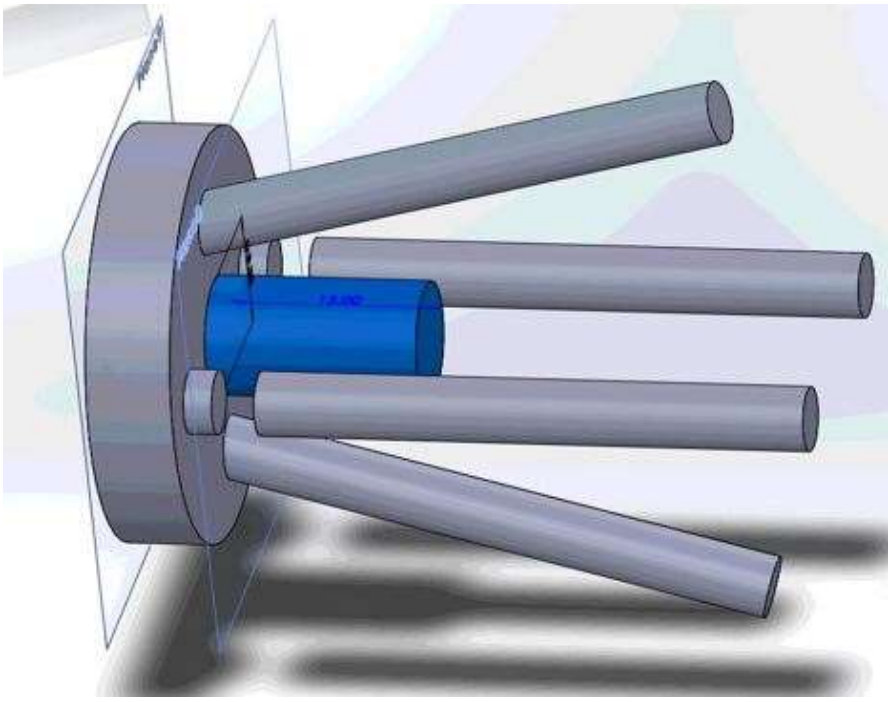

Figure 3.16: Designed baseplate with superior-inferior locking screw configuration

Regarding proper exportation from SolidWorks, two part configurations of the baseplate were required: in the basic configuration, all screws shafts were left intact; in the other, by the removal

of a 3mm gap of material from the screw shafts, compression screws were differentiated from locking screws. Sketches for the extruded cuts on the screws were made on a plane offset 2mm from the rear face of the baseplate. The reason behind this was to apply preload on the compression screws through the defined gap.

The constructed baseplate was imported into the assembly section with the scapula and the baseplates were placed on the glenoid cavity in the proper position. The glenoid cavity was then reamed similar to the conducted experiment. Using cavity feature, the scapula material was removed around the baseplate, and screws. Also, a plane offset by 50 mm was considered to shorten the scapula behind the scapular notch. The bottom face of the cavity made by the implant was used as the reference. Removing these unnecessary elements help the simulation performance and decrease computational cost. Figure 17 demonstrates the final assembly for the first model (SILS).

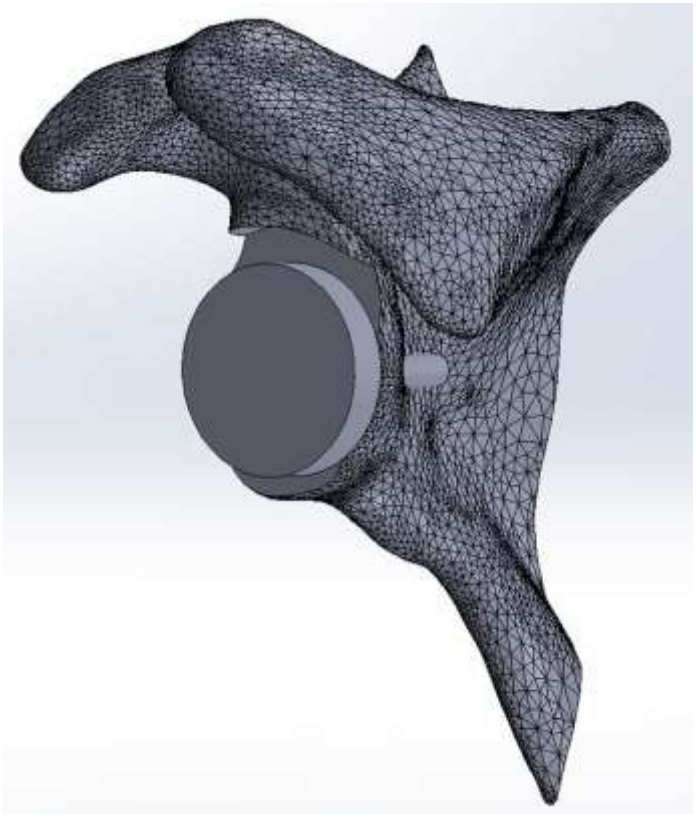

Figure 3.17: Final assembly in SolidWorks for the first model (SILS)

There are two steps for exporting the model from SolidWorks. At first, the STL files of the model with the primary baseplate configuration were exported; the scapula was saved into a specific

folder and the baseplate was deleted. Afterwards, the baseplate was changed to its new configuration with the gap between the compression screws and then the model was exported again. This time the scapula needs to be deleted and the baseplate STL file needs to be saved in that specific folder.

3.4.2.8 3matic

At the next step, the STL files were imported into 3-matic software, with a scale coefficient of millimeters and the fixed normal and split surfaces options checked. Using this software, with adaptive re-mesh feature, the scapula and baseplate were meshed with tetrahedral elements (maximum edge length of 1.6mm and preserved surface contours). And with the same maximum edge length, the volume mesh of each component were generated. Figure 19 illustrates the meshed model using 3matic.

A mesh convergence analysis was conducted using Abaqus prior to undertaking the full validation and the results showed that the best mesh size for the components would be 1.6mm. In this analysis, the mesh size was initially set at 2 mm which cause around 360 MPa of max stress. By gradually reducing the element size from 2 mm to 1.5 mm, the max stress increased from approximately 360 MPa to 1020 MPa. The maximum stress for element size 1.5 mm and 1.6 mm were basically the same. Thereby, in order to have less computational cost and simulation time, element size 1.6 mm was considered for the simulation. Figure 18 illustrates the mesh convergence analysis plot. It shows that the plot does begin to flatten out at 1.6 mm element size.

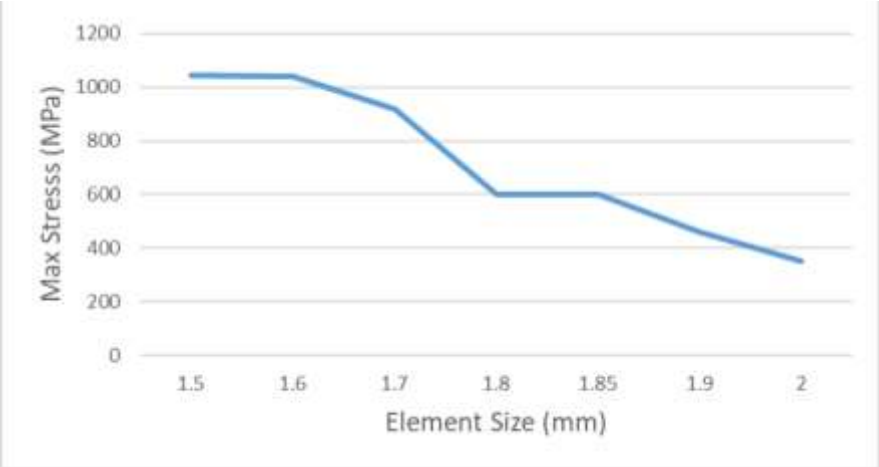

Figure 3.18: Mesh convergence analysis

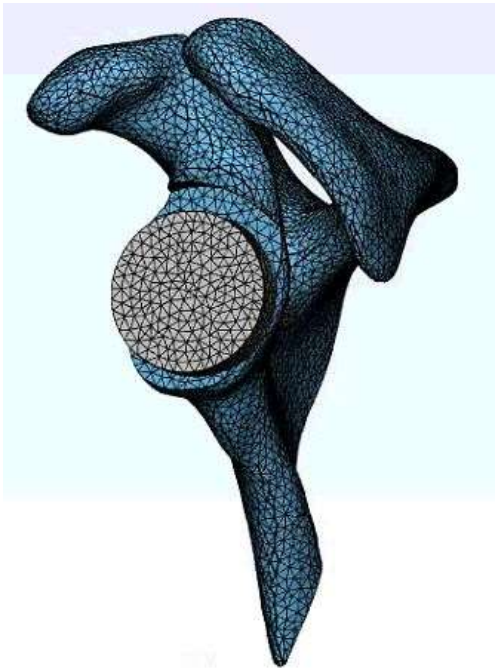

Figure 3.19: Meshed model within 3matic

To apply the heterogeneous properties to the scapula, a scapula model was copied and paste from mimics into 3-matic with the previously generated volume meshes. Two alignment tools were utilized; N-points registration, which approximately aligns the volume meshes with the imported scapula from mimics as a fix entity. The alignment will be completed using several consecutive global alignment feature. Then, the volume meshes were copied and pasted into the finite element section of mimics to apply the properties.

3.4.3 ABAQUS software

3.4.3.1 Abaqus/CAE Introduction

ABAQUS/CAE is considered as a sophisticated software which is divided into number of modules. The software provides an interface for creating, submitting, monitoring, and evaluating results from ABAQUS/standard and ABAQUS/explicit simulations. ABAQUS has all the necessary tools regarding the modelling process such as pre-processing (it provides some tools to define the geometry and material properties), processing and post-processing. The ABAQUS/CAE modules provides input files to the ABAQUS /Standard or ABAQUS /explicit analysis product (processing part). The analysis product performs the analytical process and then sends information to ABAQUS /CAE to allow in monitoring the progress of the job, and generates an output database

for post processing. At the end, ABAQUS/viewer, with different license, conducts the visualization module of ABAQUS /CAE interface. This part illustrates the graphical analysis results. Solving problems by applying finite element method has three basic steps; model creation, solution, and results interpretation and validation.

3.4.3.2 Finite Element Analysis Technique

Finite element analysis (FEA) is a numerical method which provides solutions to problems that would otherwise be difficult to obtain. In terms of fracture, FEA most often involves the determination of stress intensity factors. FEA, however, has applications in a much broader range of areas; for example, fluid flow and heat transfer. The process of finite element analysis begins with dividing the solution domain into discrete regions, termed finite elements that are interconnected at nodal points. The basic assumption in the displacement based finite element approach is to establish a set of functions that are chosen so that they uniquely define the state of displacement within each element in terms of its nodal values. In this way the number of degrees of freedom becomes finite, and any other displacement within an element can be interpolated using these so called shape functions and the known nodal values (ABAQUS 6.9 user manual, 2009).

3.4.3.3 Unit System Within Abaqus

It is essential that the units are consistent throughout the modelling in ABAQUS as there are no inherent units for ABAQUS. In the current study, the model has length in units of mm therefore the remaining units follow the highlighted column illustrated below in Table 3.1.

Table 3.1: Unit System in Abaqus Software

Quantity	SI	SI(mm)	US Unit (ft)	US Unit (inch)
Length	M	mm	ft	In
Force	N	N	lbf	Lbf
Mass	Kg	Tonne(10^3kg)	Slug	lbf s^2/in
Time	s	s	s	S
Stress	Pa (N/m^2)	MPa (N/mm^2)	Lbf/ft^2	Psi (lbf/in^2)
Energy	J	mJ (10^{-3}J)	ft lbf	In lbf
Density	Kg/m^3	$Tonne/mm^3$	$Slug/ft^3$	Lbf s^2/in^4

3.4.4 Methodology

The .inp files of volume meshes with defined material properties were exported from Mimics and then imported into ABAQUS as models. The model will be ready for processing the finite element analysis afterwards.

In the GUI of this software, the homogeneous material properties were applied to the baseplate. A young's modulus of E = 113.8 GPa and poisson's ratio of ν = 0.34 was assigned to the titanium baseplate. (http://asm.matweb.com).

The boundary condition was defined like the way the scapula were fixed similar to the experiment. The encastre boundary condition was used to fix the chosen face in all degree of freedom consistent with the experimental set-up.

Table 2 illustrates the interaction properties applied at the proper components' interfaces.

Table 3.2: Defined interaction properties for appropriate interfaces

Interaction	Property
Screw-bone	μ = Tied [MacLeod et al.]
Implant-bone (Ti-bone)	μ = 0.74 [Zhang et al.]

Regarding the compression screw design, it was assumed that there was no rotation relative to the baseplate. Specifically, as mentioned at the beginning of this section, in the physical system there are rotational degree of freedom (DOF) in the compression screw-baseplate interaction which are only restricted by friction. However, because the compression load is high enough, it was assumed that the friction is adequate to allow an assumption of negligible rotation between the two parts. Therefore, the rotational degree of freedom restriction could be ignored by integrating the compression screw heads with the baseplate. To define the compression screws attached to the baseplate a preload force was considered between the two sections of the compression screws with the bushing connector feature in the software. Dharia et al. determined a value of 627 N for the preload in compression screws which their results were more applicable. As illustrated in figure 20, two behavior options were defined for the bushing connector; a stiffness D_{33} = 627 N/mm and a reference length of 2 mm which connected two arbitrary collinear mesh nodes on either side of the gap at the predefined 3 mm gap in the compression screws.

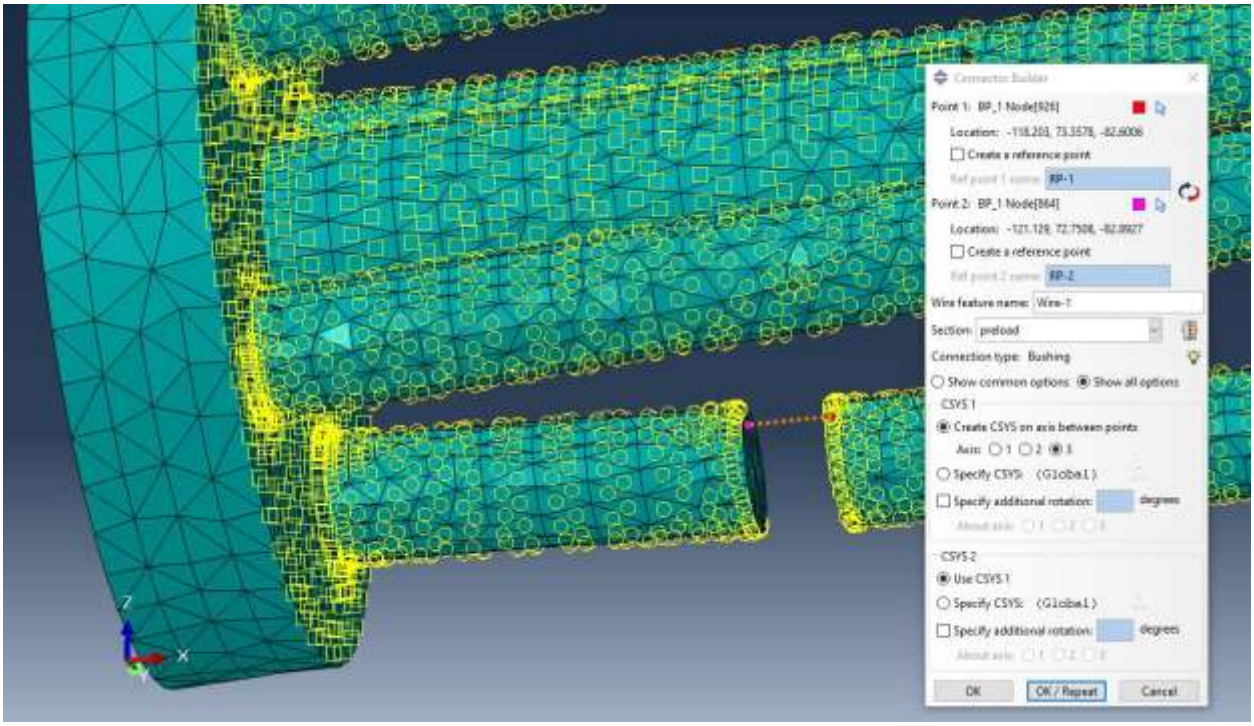

Figure 3.20: Connector feature and end-points selected as collinear mesh nodes on either side of the gap

In the load section, instead of a load with an eccentricity, an equivalent load perpendicular to the baseplate surface and an equivalent moment about the positive x-axis were applied to the baseplate

center similar to the experiment. The coupling feature was defined for the model prior to apply the equivalent moment. Figure 21 illustrates the direction of the equivalent load and moment.

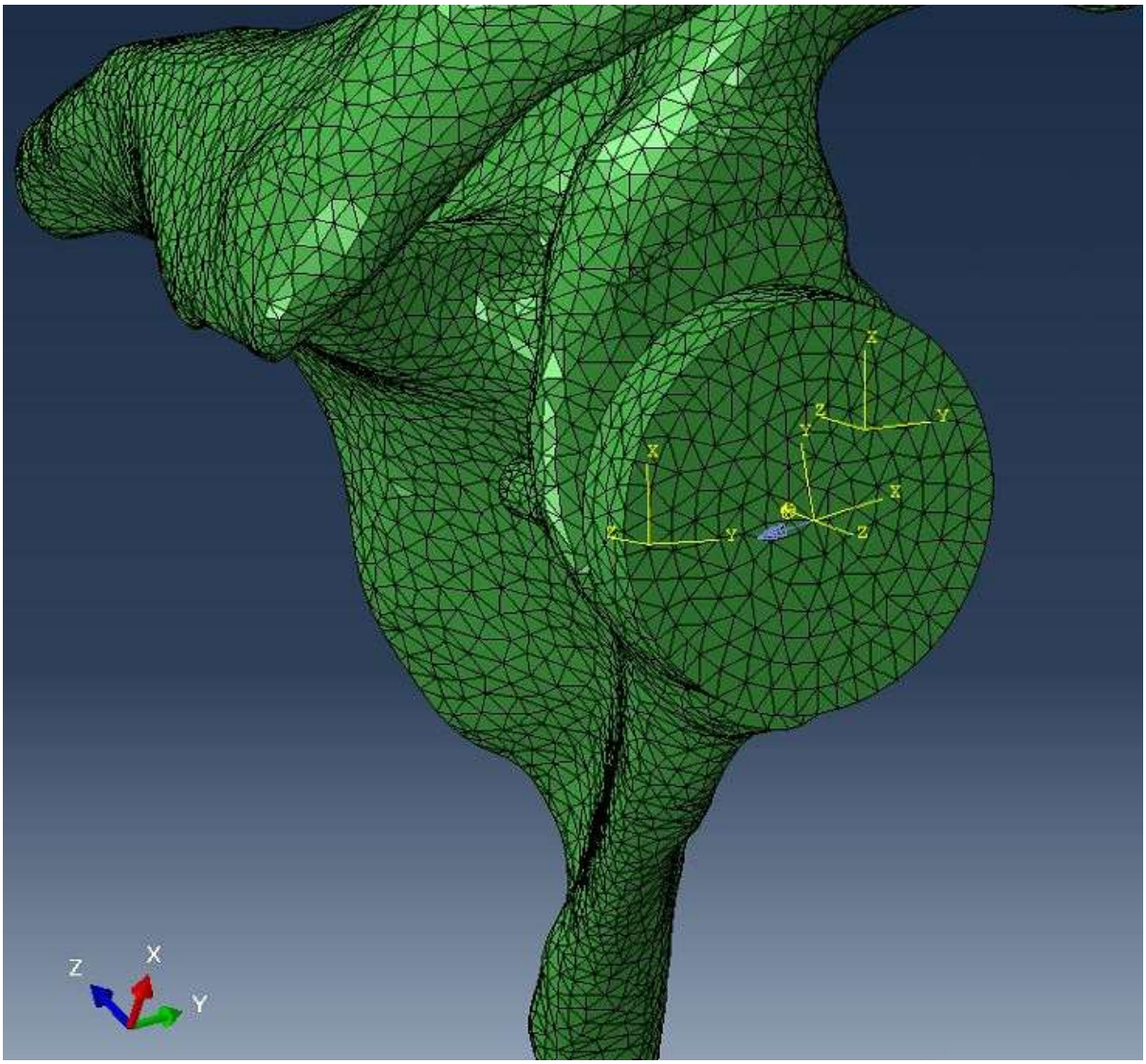

Figure 3.21: Direction of the equivalent load and moment

Figure 22 illustrates the schematic representation of the test apparatus and the simulation study. Basically, this picture depicts what was conducted in the experimental study and efforts were made to replicated these conditions in the simulations.

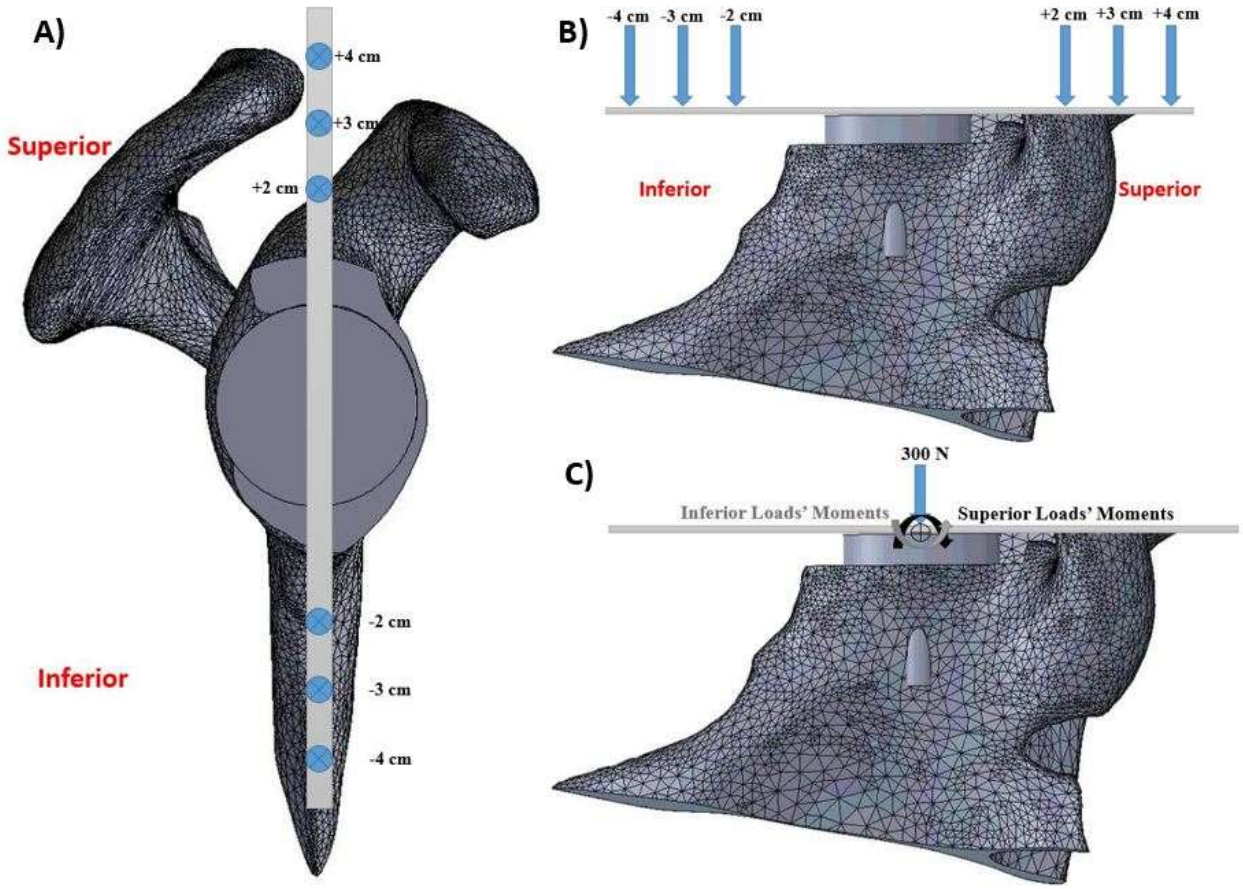

Figure 3.22: Applied load with different superior and inferior eccentricities on the rigid body the exact way it was done at the experimental study in A) Front and the B) Side view, C) Applied equivalent load and moment on the baseplate.

Using the baseplate diameter of 29mm, table 3 demonstrates the equivalent force and moment applied on the baseplate center for each eccentricity; superior and inferior eccentricities are shown with positive and negative numbers respectively.

Table 3.3: Equivalent force and moment applied on the baseplate center

Force (N)	Eccentricity (cm)	Equivalent Moment (N.mm)
150	±2	±5175
	±3	±6675
	±4	±8175
300	±2	±10350
	±3	±13350
	±4	±16350

Finally, the simulations were run and the results were acquired by measuring the nodes micromotion and displacements. When the load was applied superiorly, the node micromotion at the inferior edge of the baseplate was measured and when the load was applied inferiorly, the node micromotion at the superior edge of the baseplate was measured at the end of the simulation while the load was being applied. This was done to match the experimental method; when the loads were applied by superior and inferior eccentricity, the micro motion of the inferior and superior edge of the baseplate were measured respectively. One of the assumptions that was considered during the simulation was that each nodal micromotion measurement was extracted for 150 N and 300 N without considering the bone fatigue. However, in the experiment, each bone underwent repeated, increasing loading which may have caused permanent deformation to the implant configuration. As an example, in the experiment, after applying 50 N load to the specimen, the bone deforms slightly and then having that previous deformation, goes under 100 N load. On the other hand, in the simulation, the bone underwent 150 N and 300 N load once from the original unloaded configuration. This may affect the accuracy of the simulation results as at some certain previous loads the scapula bone might deform permanently. Moreover, it is worth to mention that in the experiment, LVDT sensor measured the displacement merely before and after the load was applied. Thus, the sensor could not detect any previous plastic deformation from former loads. There is another potential uncertainty about the result simulation. As it is mentioned before, in the experiment the forces were applied on the rigid body at their exact eccentricities, however, in the simulation using the couple feature in ABAQUS software, the equivalent forces and moments were applied on the baseplate center which add a bit of simplicity to the simulation as the coupling feature helps to constrain one surface movement to one node. ABAQUS is a finite element software and solve the problems element by element and coupling feature basically simulate and consider a surface with a node. So, using couple feature to simulate the equivalent load and moment instead of applying the load at its eccentricity is a simplification and might slightly affect the results

3.5 Summary

In this chapter the methodology of the data processing during the project was described.

There is some software that were utilized during the project such as SolidWorks, Mimics, 3-matic, and ABAQUS. The main applications were ABAQUS and Mimics. Using Mimics, the segmentation of the bone from other parts such as tissues, ligaments, muscles, and skin was done. Afterwards, the 3-D geometry of the bone component which is scapula in this case, was acquired.

The ABAQUS software is utilized for conducting finite element analysis on the model and again apply the necessary modification and requirements to enable the software to run the finite element analysis on the created implant parts with the scapula bone.

In the next chapter the complete altered model that was imported into ABAQUS will be used in the finite element analysis. The displacements and deformations of the bone-implant interface will be analyzed using finite element analysis to assess the reverse total shoulder implant effectiveness on the patient that already underwent the surgery during daily life activities.

Chapter 4. Results

After running the simulations, the results and data were extracted from Abaqus and imported into Excel software to analyze the results and producing the graphs. Afterwards, the data were imported into SPSS software to conduct the statistical analysis.

The data averages of the six models and the standard deviations were calculated within Excel. Finally, four average plots were extracted. These plots illustrate the micromotion-eccentricity relation when you apply 150N and 300N on six different eccentricities; superior (+2, +3, and +4 cm) and inferior (-2, -3, and -4 cm).

Mathematically speaking, by increasing the eccentricity, the micromotion in the other baseplate edge should increase owing to the fact that the moment arm (distance of the force to the point we calculate the moment) and consequently the moment increases. This rule is strictly enforced in the simulations and observed in the simulation results for all the models and averages, which helps to verify the validity of the simulation results. This rule is largely followed by the experimental results but the issues previously described regarding permanent deformation and the use of .LVDTs leads to some deviation from this rule.

Figure 1 demonstrates the average baseplate micromotion for simulation and experiment when we applied the load equal to 150N on 2, 3, and 4cm superior eccentricity.

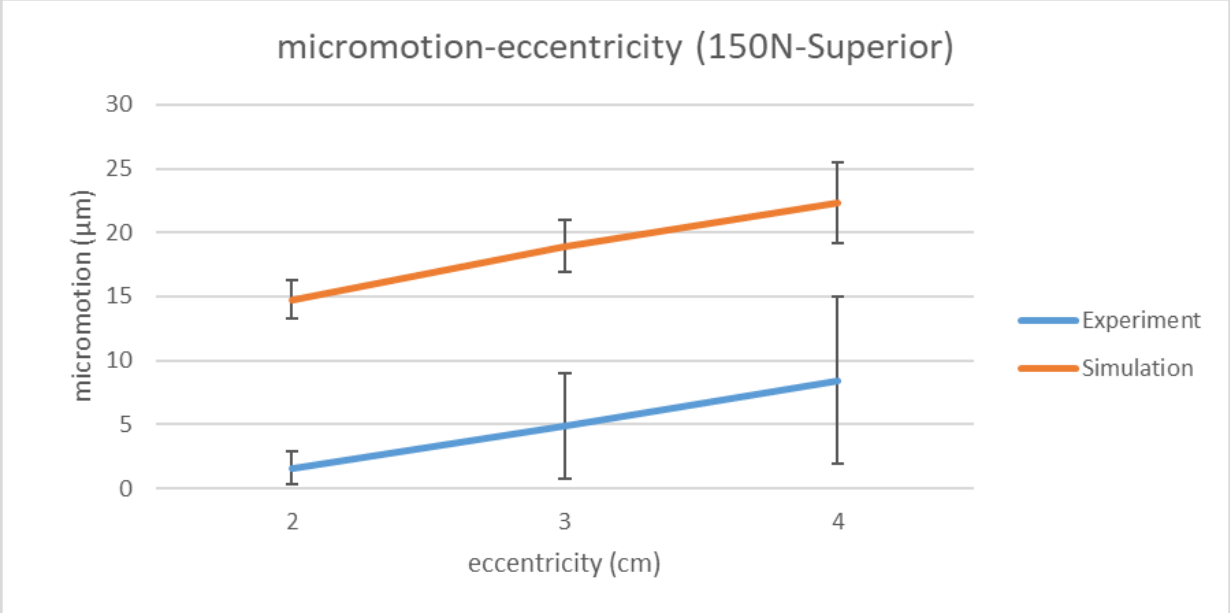

Figure 4.1: Average baseplate micromotion for simulation and experiment when we applied the load equal to 150N on 2, 3, and 4cm superior eccentricity

Considering the graph, for simulation and experimental results the baseplate micromotion is increasing by increasing the eccentricity from 2 to 4 cm. Therefore, the trends for the experimental and simulation results are the same. Also, by increasing the eccentricity, the standard deviation of the results is increasing.

Figure 2 illustrates the average micromotion of the baseplate for experimental and simulation results when 300N load was applied on 2, 3, and 4cm eccentricities superiorly.

As it is shown in the graph, by increasing the eccentricity from 2 to 4 cm, the baseplate micromotion of the simulation and experimental results is increased from 22.52 to 36.04 µm and 10.8 to 13.86 µm respectively. Therefore, the trends for the experimental and simulation results are the same. Also, by increasing the eccentricity, the standard deviation of the results is increasing. However, the standard deviation for experimental results are higher compare to the simulation results. It means that the dispersion of the dataset relative to its mean for the experimental results are higher than simulation results.

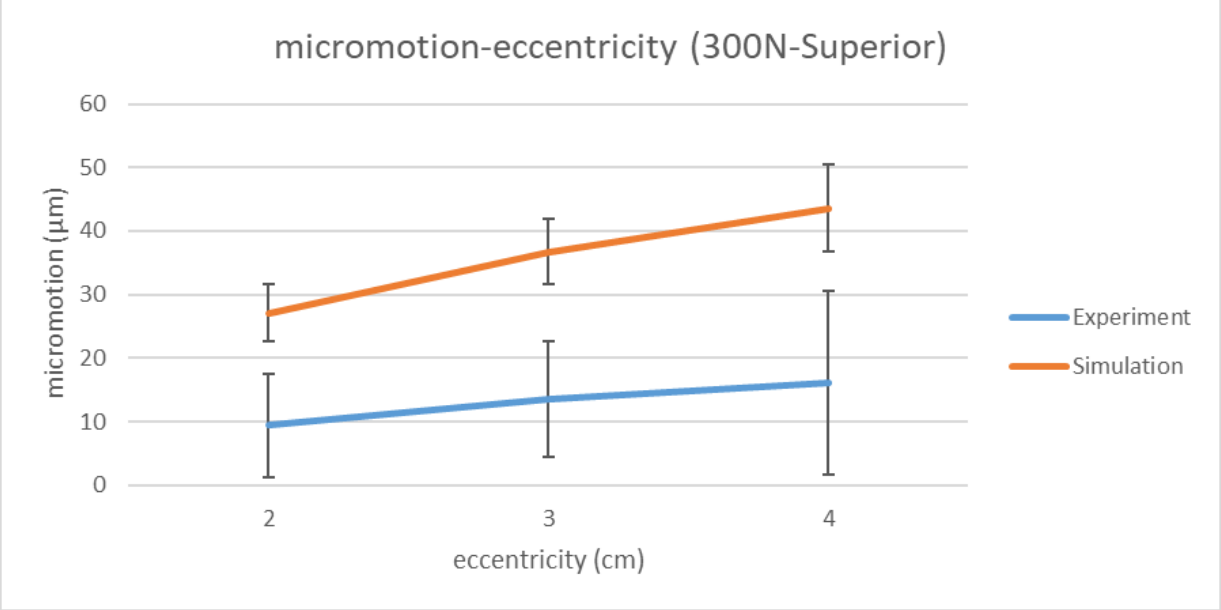

Figure 4.2: The average micromotion of the baseplate for experimental and simulation results when we applied 300N load on 2, 3, and 4cm eccentricities superiorly

Another verification of the simulation results is by increasing the load from 150N to 300N, the micromotion of the baseplate was increased which is reasonable as by increasing the load, the moment will be increased and therefore cause more displacement of the nodes. Figure 3 shows the micromotion-eccentricity when 150N and 300N is applied on the baseplate with superior and inferior eccentricities.

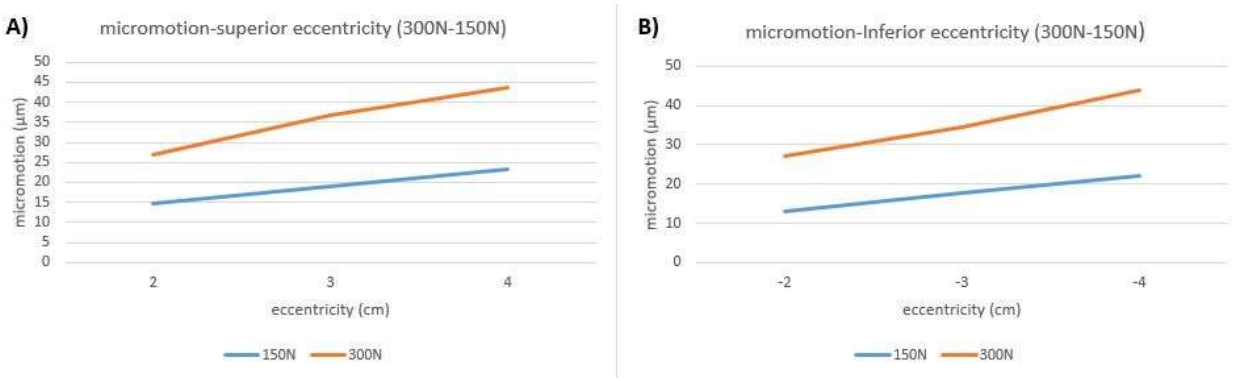

Figure 4.3: micromotion-eccentricity when 150N and 300N is applied on the baseplate with A) superior and B) inferior eccentricities.

Figure 4 shows the average baseplate micromotion for simulation and experimental results when the load equal to 150N was applied on 2, 3, and 4cm inferior to the inferior edge of the baseplate.

The graph demonstrates that for the simulation results the baseplate micromotion is increasing by increasing the eccentricity from 2 to 4 cm. However, for the experimental results, the micromition is decreased by increasing the eccentricity from 2 to 3 cm but afterwards by increasing the eccentricity from 3 to 4 cm, the micromotion is increased by the same trend as the simulation graph. This discrepancy might have happened because of some reasons such as: the baseplate fixation at the experiment, the bone poor quality of a scapula sample that was undertaken through the mechanical tests, and any bone breaks or cracks in a scapula bone specimen. Furthermore, the model number four was reamed more inferiorly compare to the other models and what it supposed to be, which has effected on the results too. Also, by increasing the eccentricity, the standard deviation of the results is increasing. the standard deviation (SD) for experimental results are higher compare to the simulation results. It means that the dispersion of the dataset relative to its mean for the experimental results are higher than simulation results.

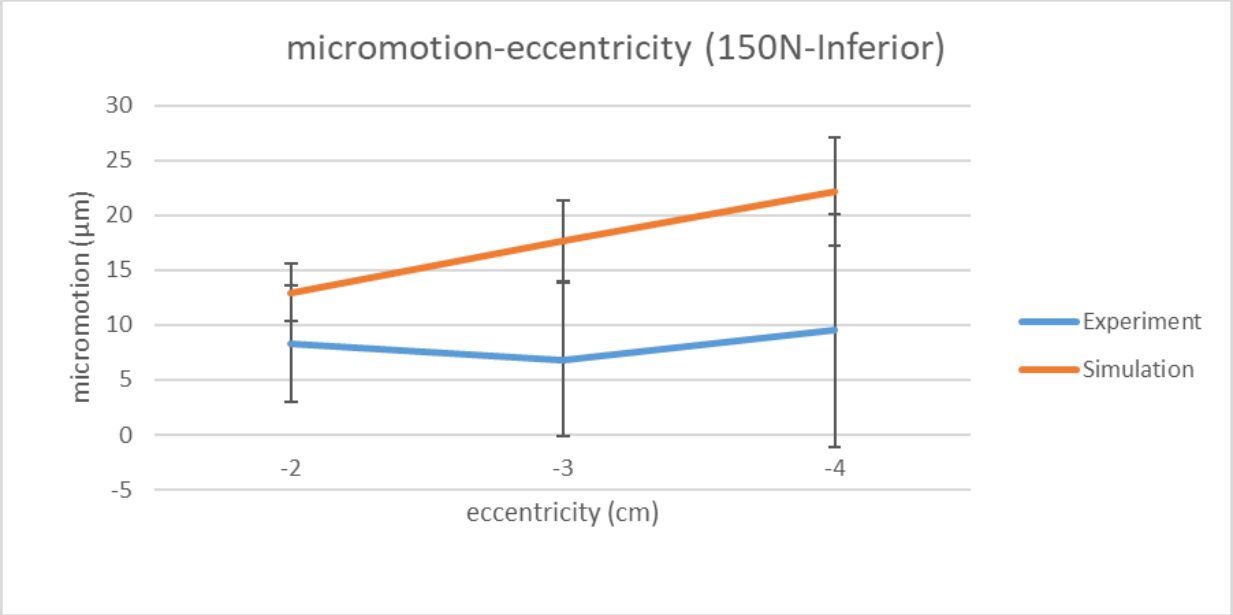

Figure 4.4: the average baseplate micromotion for simulation and experimental results when we applied the load equal to 150N on 2, 3, and 4cm inferior to the inferior edge of the baseplate.

Figure 5 demonstrates the baseplate average micromotion for simulation and experimental results when the load equal to 300N was applied on 2, 3, and 4cm eccentricities inferiorly.

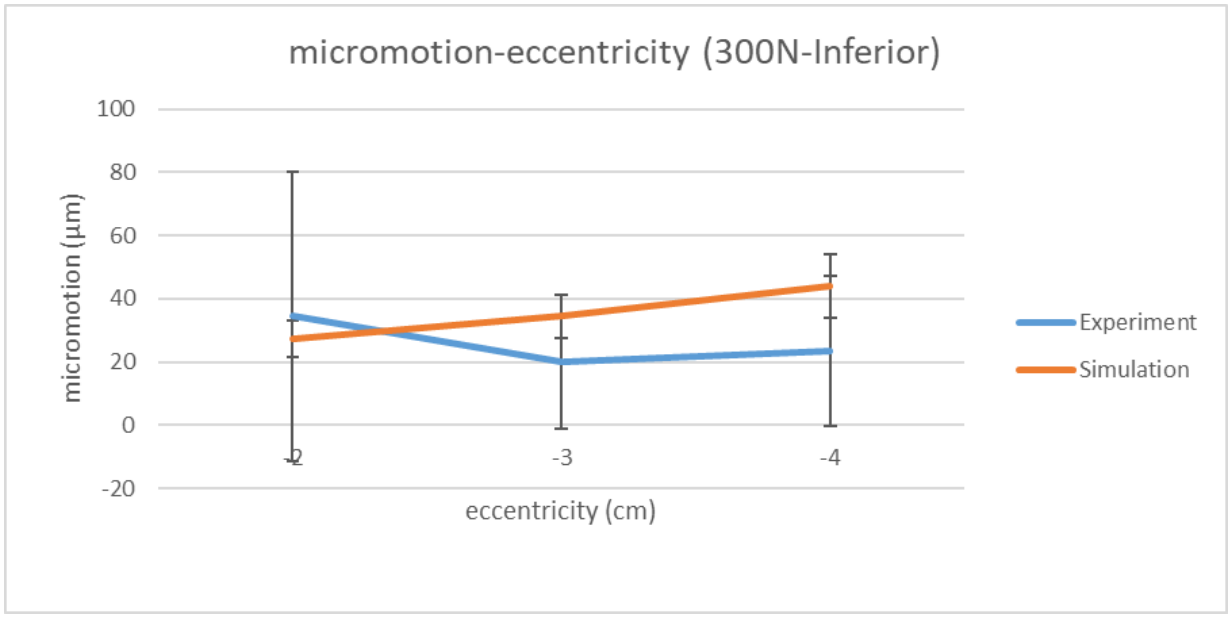

Figure 4.5: the baseplate average micromotion for simulation and experimental results when we applied the load equal to 300N on 2, 3, and 4cm eccentricities inferiorly.

It shows that for the simulation results, similar to the other plot, the baseplate micromotion is increasing from 21.003 to 33.78 µm by increasing the eccentricity from 2 to 4 cm respectively

which is reasonable and shows the verification of the simulation results. However, for the experimental results, by increasing the eccentricity from 2 to 3 cm the micromition is decreased from 30.91 to 17.71 µm, but is increased afterwards again from 17.71 to 20.49 µm by increasing the eccentricity from 3 to 4 cm with the same trend as the simulation graph. This discrepancy might have happened because of some reasons such as: the baseplate fixation at the experiment, the bone poor quality of a scapula sample that was undertaken through the mechanical tests, and any bone breaks or cracks in a scapula bone specimen. Furthermore, the model number four was reamed more inferiorly compare to the other models and what it supposed to be, which has effected on the results too. Furthermore, in this plot similar to the other, by increasing the eccentricity from 2 to 3 cm, the standard deviation is decreased but from 3 to 4 cm, the standard deviation of the results is increasing. The standard deviation for experimental results are higher compare to the simulation results. It means that the dispersion of the dataset relative to its mean for the experimental results are higher than simulation results.

It is worth mentioning that because the trends of both the simulation and experimental results are similar, the simulation mechanics can be considered to be adequately modelled; by mechanics it means the defined general contacts and interactions between various parts of the model. By increasing the load eccentricities, the node micromotion in both simulation and experimental results were increased. This means that in the simulation the model constituents were properly assembled and considering the proper general contact and interaction properties, the load was decently distributed between each component.

Statistical analysis was conducted on the results of the six models for the experimental and simulation results. A two-way ANOVA was conducted to determine the effects of test-method and eccentricity on baseplate micromotions. Data are mean ± standard deviation, unless otherwise stated. Residual analysis was performed to test for the assumptions of the two-way ANOVA. There were no outliers, as assessed by inspection of a boxplot. micromotions were normally distributed for the experimental and simulation as assessed by Shapiro-Wilk's test of normality ($p > 0.05$). There was a statistically significant interaction between eccentricity and test-method on baseplate micromotions, $F(5,25) = 3.375$, $p = 0.018 < 0.05$. Therefore, an analysis of simple main effects for eccentricity was performed with statistical significance receiving a Bonferroni adjustment and being accepted at the $p < 0.025$. There was a statistically significant simple simple main effect of

eccentricity for simulations results ($F(5, 25) = 10.627$, $p = 0.000 < 0.05$), but not for experiments results ($F(5, 25) = 0.622$, $p = 0.530 > 0.05$) on the baseplate micromotion. Thus, micromotion changes by eccentricity for the simulation results but not for experimental results. Data are mean ± standard deviation, unless otherwise stated. When 300N load was applied, the mean "micromotion" for simulations was 33.0963 ± 8.4 and 15.3599 ± 13.5 for experiments.

Chapter 5. Discussion

The results of the simulation and the experimental study were fairly similar to each other. However, it is worth mentioning that since the trend of the results match the experiments as elaborated on in the result section, the overall mechanics were properly modelled. This means that in the simulation the model constituents were properly assembled and considering the proper general contact and interaction properties, the load was decently distributed between each component.

However, there is a potential uncertainty about the result simulation. As it is mentioned before in the experiment the forces were applied on the rigid body at their exact eccentricities, however, in the simulation using the couple feature in Abaqus software, the equivalent forces and moments were applied on the baseplate center. As it is mentioned earlier, the coupling feature helps to constrain one surface movement to one node. Also, ABAQUS is a finite element software and solve the problems element by element. Coupling feature basically simulate and consider a surface with a node. So, using couple feature to simulate the equivalent load and moment instead of applying the load at its eccentricity is a simplification which might add a bit of additional uncertainty to the simulation.

An additional assumption in this study was that there is high enough compression of the compression screws to neglect their free rotational degrees of freedom (DOF) with the baseplate. Specifically, at the compression screw-baseplate interaction there are rotational degree of freedom which are only restricted by friction. Owing to the fact that the compression load is high enough, it was assumed that the friction is adequate and also there is a small rotation between the two parts. Therefore, the rotational degree of freedom restriction could be assumed and thus integrating the compression screw heads with the baseplate was modeled.

In this study the finest mesh was applied in 3-matic software, the heterogeneous mechanical properties were applied to the scapula using Calibration Phantom which is a precise method, also, the preload was applied for the compression screws. However, in order to get more accurate results, we can increase the accuracy of the experimental setup and scapula fixations. Bone specimens with improved bone material properties would enable an improved match between the simulations and experiment. Specifically, some specimens in this study had poor bone quality, which may have

led to permanent deformation during low level loading, which would have skewed the experimental deformation results at higher load levels. These skewed deformations would not align with the simulations where permanent deformations in low load simulations would not be accounted for in the higher critical loading cases. Moreover, considering the reasons that are already mentioned, the exact force in its eccentric position instead of modeling an equivalent force and moment could improve the results' accuracy. Finally, more experimental data and pictures were needed in order to analyze and compare with the simulation results. More experimental data would make our study more statistically valid and likely to represent the true population. In addition, having more pictures of the experimental setup helps in different ways in order to enhance the simulation results. By having more pictures of the experimental setup, it would be possible for us to more accurately match our simulations with regards to how the scapula bones were fixed using plaster and the exact technique used to ream the glenoid bone. Also, one of the important sections in the simulation was adjusting the baseplate with the reamed scapula which was done in SolidWorks and obviously has a large effect on the results. Having access to more pictures from different views of the experiments could profoundly improve the model accuracy and yield improved results.

There are some deviations between the experimental and simulation results. These discrepancies might have happened due to some reasons such as: the baseplate adjustment. As was mentioned earlier, the baseplate fixation was a crucial part of the simulation where adjustments to the baseplate fixation could positively or adversely affect all the contact and interaction properties. Thereby, any difference between the experimental and simulation baseplate fixation can cause high discrepancies in results. Furthermore, the poor bone quality of a scapula sample that was undertaken through the mechanical tests might be a source of inconsistency between the experimental and simulation result. Plus, any bone breaks or cracks in a scapula specimen could adversely affect the results. As an example, if in the experiment a bone specimen contained cracks or other areas of weakness, at the beginning the bone acts normally but at a certain force the crack may prorogate and cause permanent deformation. An another issue could be that whereas the models assume perfect contact between the baseplate and bone, in reality there may be a small gap that closes and permanently deforms after initial loading. Neither of the types of permanent deformation would be detected by our simulations. Also, considering the pictures from the experiment provided by Western University, the model number four was reamed more inferiorly

compare to the other models and what is standard clinical practice, which could affect results by influencing the contact and interaction properties between the baseplate and the scapula bone. Furthermore, as was mentioned in section 3, one of the assumptions that was considered during the simulation was that each nodal micromotion measurement was extracted for 150 N and 300 N without considering the bone fatigue. However, in the experiment, each bone underwent progressively increase loads. Each of the above factors contribute to the discrepancies between the experimental and simulation results.

Chapter 6. Conclusion

A workflow has been utilized in the current study in order to develop and improve the finite element analysis of a prosthesis and to optimize the implants' design. The overall objective of this study was to find out whether this workflow is accurate enough in order to address clinical questions about reverse prosthesis design. To do so, the simulation was done using this procedure and the results were compared to an experiment that was conducted by colleagues in Western University, Ontario, Canada.

Five software were used in this workflow; ABAQUS 2019 (Dassault Systèmes, Vélizy-Villacoublay, France), SolidWorks 2018 (Dassault Systèmes, Vélizy-Villacoublay, France), Mimics 21.0 (Materialise, Leuven, Belgium), 3Matics (Materialise, Leuven, Belgium), and SPSS. The 3-D bone geometries were produced from CT-scan images using Mimics. The implant design, its assembly with the scapula, and trimming the scapula similar to the experiment were done using SolidWorks. The model then imported to Mimics in order to apply the proper mesh configuration. Afterwards, the model was taken into Mimics again for applying the heterogenous mechanical properties on the scapula. The whole model with all components were then imported into ABAQUS software. After defining boundary conditions, loads and moments, screw preload, and constraints similar to the experiment, the finite element analysis was done in order to get the dislocation results. Finally, the results were then compared with the experimental study using SPSS software.

The models were found to follow the expected trends of the mechanics and what was seen in the experimental data and thus the modeling workflow makes sense overall. However, it needs further refinement to calibrate the models before it could be utilized in order to answer clinical questions.

Overall, the study results could be valuable in order to do more accurate finite element analysis and this can be helpful for prosthesis designers to optimize and improve the implant designs.

References

- Barnett CH, Davies DV, MacConnail MA. Synovial joints: their structure and mechanics. Synovial joints: 1961.

- Buchler, P., Ramaniraka, N. A., Rakotomanana, L. R., Iannotti, J. P., Farron, A., 2002. A finite element model of the shoulder: application to the comparison of normal and osteoarthritic joints. Clin Biomech (Bristol, Avon) 17, 630-9.

- Chadwick, E.K., van Noort, A., van der Helm, F.C., Biomechanical analysis of scapular neck malunion- a simulation study. Clinical Biomechanics, Bristol, Avon, 2004, 19(9), 906-912.

- De Wilde LF, Audenaert EA, Berghs BM. Shoulder prostheses treating cuff tear arthropathy: A comparative biomechanical study. J Orthop Res 2004; 22:1222-30.

- Denard, P. J., Lederman, E. S., Parsons, B. O., & Romeo, A. A. (2017). Finite element analysis of glenoid-sided lateralization in reverse shoulder arthroplasty. Journal of Shoulder and Elbow Surgery, 26(10), e319. doi: 10.1016/j.jse.2017.06.008

- Frankle M, Siegal S, Pupello D, Saleem A, Migheli M, Vasey M. The reverse shoulder prosthesis for glenohumeral arthritis associated with severe rotator cuff deficiency: A minimum two year follow up study of sixty patients. J Bone Joint Surg Am 2005; 87:1697-705.

- Frederick A. Matsen, III, Pascal Boileau, Gilles Walch, Christian Gerber and Ryan T. "The Reverse Total Shoulder Arthroplasty"Bicknell *J Bone Joint Surg Am.* 2007;89:660-667.

- Fu, H.F, Seel, M.J., Berger, R.A., Relevant Shoulder Biomechanics, Operative Techniques in Orthopaedics, Vol. 1, No 2 (April), 1991: PP 134-146.

- Gupta S, van der Helm FC, van Keulen F. The possibilities of uncemented glenoid component--a finite element study. Clin Biomech (Bristol, Avon). 2004 Mar;19(3):292-302. PubMed PMID: 15003345.

- Hamill, J., Knutzen, K.M., Biomechanical Basis of Human Movement, London, Williams and Wilkins, 1995.

- Harman M, Frankle M, Vasey M, Banks S. Initial glenoid component fixation in ''reverse'' total shoulder arthroplasty: a biomechanical evaluation. J Shoulder Elbow Surg 2005; 14:162-7. http://dx.doi.org/ 10.1016/j.jse.2004.09.030

- Hay, J.G., Reid, J.G., Anatomy, Mechanics, and human motion, 3rd edition, New Jersey: Prentice-Hall, 1999

- Hopkins A. R., Hansen U. N., Bull A. MJ, Emery R., Amis A.: Fixation of the reversed shoulder prosthesis. London: J Shoulder Elbow Surg, 2008.

- Katz D, O'Toole G, Cogswell L, Sauzieres P, Valenti P. A history of the reverse shoulder prosthesis. Int J Shoulder Surg 2007; 1:108-13

- Labriola, J. E., Lee, T. Q., Debski, R. E., McMahon, P. J., Stability and instability of the glenohumeral, 2005.

- M. A. Daalder, G. Venne, V. Sharma, M. Rainbow, T. Bryant, and R. T. Bicknell, "Trabecular bone density distribution in the scapula relevant to reverse shoulder arthroplasty," JSES Open Access, vol. 2, no. 3, pp. 174–181, Oct. 2018.

- M. T. Wong, G. D. G. Langohr, G. S. Athwal, and J. A. Johnson, "Implant positioning in reverse shoulder arthroplasty has an impact on acromial stresses," J. Shoulder Elb. Surg., vol. 25, no. 11, pp. 1889–1895, Nov. 2016.

- Marieb, E.N, Human Anatomy and physiology, 3rd edition, California Benjamin Cummings Publication Company, Inc 1995.

- Martini, F.H., Ober, W.C., Garrison, C.W., Welch, K, Hutchings, R.T, Fundamentals of Anatomy and Physiology, 5th edition, New Jersey: Prentice-Hall, Inc, 2001.

- McFarland E.G, Sanguanjit P, Tasaki A, Keyurapan E, Fishman E.K, Fayad L.M, The reverse shoulder prosthesis: a review of imaging features and complications, Skeletal Radiol (2006) 35:488-496 DOI 10.1007/s00256-006-0109-1

- Nazeem A. Virani MDa, Melinda Harman MScb, Ke Li PhDc, Jonathan Levy MDd, Derek R. Pupello MBAa, Mark A. Frankle MDe, In vitro and finite element analysis of glenoid bone/baseplate interaction in the reverse shoulder design, Journal of Shoulder and Elbow Surgery, Volume 17, Issue 3, May-June 2008, Pages 509-521

- Neer C.S.and Morrison D.S., Glenoid bone-grafting in total shoulder arthroplasty. *J. Bone Joint Surg. Am.*, 70 (1988), pp. 1154–1162.

- Neer CS 2nd, Watson KC, Stanton FJ. Recent experience in total shoulder replacement. J Bone Joint Surg Am 1982; 64:319-37.

- Nyffeler RW, Werner CM, Simmen BR, Gerber C. Analysis of a retrieved Delta III total shoulder prosthesis. J Bone Joint Surg Br 2004; 86:1187-91.

- Reeves B, Jobbins B, Dowson D, Wright V. A total shoulder endoprosthesis. Eng Med. 1974;1: 64–67.

- Reeves B, Jobbins B, Flowers F, Dowson D, Wright V. Biomechanical problems in the development of a total shoulder endo-prosthesis. Ann Rheum Dis. 1972; 31:425–426.

- Roetert, E. P., Shouldering the Load, Strength and Conditioning Journal 25(1):20-21, 2003.

- Schiffern S.C., Rozencwaig R, Antoniou J, Richardson M.L., Matsen F.A., 3rd, Anteroposterior centring of the humeral head on the glenoid in vivo. Am. J. Sports Med. 2002; 30: 382-7.

- Sirveaux F., Favard L., Oudet D., Huquet D., Walch G, Mole D., Grammont inverted total shoulder arthroplasty in the treatment of glenohumeral osteoarthritis with massive rupture of the cuff. Results of a multicentre study of 80 shoulders. Journal of Bone Joint Surgery 2004; 86:388-395.

- Valenti P, Boutens D, Nerot C. DELTA III reversed prosthesis for osteoarthritis with massive rotator cuff tear: Long term results (>5 years). *In:* Walch G, Mole D, editors. 2000 shoulder prostheses. Two to Ten years follow. Sauramp Medical: Montpellier; 2001. p. 253-9

- Werner CM, Steinmann PA, Gilbart M, Gerber C. Treatment of painful pseudoparesis due to irreparable rotator cuff dysfunction with the Delta III reverse-ball-and-socket total shoulder prosthesis. J Bone Joint Surg Am. 2005; 87:1476–1486.

- Wirth M, Rockwood CA Jr. Current concept review: Complications of total shoulder replacement arthroplasty. J Bone Joint Surg Am 1996; 78:603-16.

- Yang, C.-C., Lu, C.-L., Wu, C.-H., Wu, J.-J., Huang, T.-L., Chen, R., & Yeh, M.-K. (2013). Stress analysis of glenoid component in design of reverse shoulder prosthesis using finite element method. *Journal of Shoulder and Elbow Surgery*, *22*(7), 932–939. https://doi.org/10.1016/j.jse.2012.09.001

- Yokochi, C., Rohen, J.W., Weinreb, E.L., Photographic Anatomy of the Human Body, 3rd edition, Tokyo: Igaku-Shoin.

- Wright medical: Bony increased oset-reverse shoulder arthroplasty, http: / / www. wright. com / products - upper / bio - rsa - bony - increased - offset - reversed - shoulder-arthroplasty, Accessed: 2020-04-23.

- J. M. Reeves, G. S. Athwal, and J. A. Johnson, \An assessment of proximal humerus density with reference to stemless implants", Journal of shoulder and elbow surgery, vol. 27, no. 4, pp. 641{649, 2018.

- Asm aerospace specification metals inc. http://asm.matweb.com/search/SpecificMaterial. asp?bassnum=MTP641, Accessed: 2020-04-24.

- R. MacLeod, P. Pankaj, and A. H. R. Simpson, \Does screw {bone interface modelling matter in finite element analyses?", Journal of biomechanics, vol. 45, no. 9, pp. 1712{1716, 2012.

- Y. Zhang, P. B. Ahn, D. C. Fitzpatrick, A. D. Heiner, R. A. Poggie, and T. D. Brown, \Interfacial frictional behavior: Cancellous bone, cortical bone, and a novel porous tantalum biomaterial", Journal of Musculoskeletal Research, vol. 3, no. 04, pp. 245{ 251, 1999.

- M. D. Mahaffy, \Examining reverse total shoulder arthroplasty baseplate fixation in patients with e2-type glenoid erosion", 2018.

- C. Studders, D. Saliken, H. Shirzadi, G. Athwal, and J. Giles, \Impact of screw configuration on graft micromotion in bony increased offset-reverse shoulder arthroplasty applied to the b2 glenoid", in Orthopaedic Proceedings, The British Editorial Society of Bone & Joint Surgery, vol. 102, 2020, pp. 41-41.

- M. Dharia and S. Mani, \Impact of screw preload on primary stability in reverse shoulder arthroplasty", in Orthopaedic Proceedings, The British Editorial Society of Bone & Joint Surgery, vol. 101, 2019, pp. 48{48.

- Werner Pomwenger*, Karl Entacher, Herbert Resch and Peter Schuller-Götzburg\ “Need for CT-based bone density modelling in finite element analysis of a shoulder arthroplasty revealed through a novel method for result analysis”, in Biomed Tech 2014; 59(5): 421–430.

- Andrew S, Michalskia b, Bryce A. Beslera b, Geoffrey J, Michalaka b, Steven K\ “CT-based internal density calibration for opportunistic skeletal assessment using abdominal CT scans” in Medical Engineering and Physics, 78(2020)55–63.

- Jonathan Kusins, Nikolas Knowlesa, Melissa Ryanc, Enrico Dall’Arac, Louis Ferreira\ “Performance of QCT-Derived scapula finite element models in predictinglocal displacements using digital volume correlation” in Journal of the Mechanical Behavior of Biomedical Materials 97 (2019) 339–345.

- S Abdic, J Lockhart, N Alnusif, J Johnson, G Athwal, “Glenoid Baseplate Screw Fixation in Reverse Shoulder Arthroplasty: Does Locking Screw Position and Orientation Matter?”

Appendix A:

Abduction: A movement away from the midline of the body.

Absolute Reference Frame: A reference frame in which the origin is at the joint center.

Adduction: A movement toward the midline of the body.

Anatomical Position: The standardized reference position used in the medical profession.

Anatomy: The science of the structure of the body.

Angular Motion: Motion around an axis of rotation in which different regions of the same object do not move through the same distance.

Anterior: A position in front of a designated reference point.

Anteroposterior Axis: The axis through the center of mass of the body running from posterior to anterior.

Axis: The imaginary line of a reference system along which position is measured.

Axial Skeleton: The bones of the head, neck, and trunk.

Axis of Rotation: The imaginary line about which an object rotates.

Biomechanics: The study of motion and the effect of forces on biological systems.

Cardinal Planes: The planes of the body that intersect at the total body center of mass.

Circumduction: A movement that is a combination of flexion, adduction, extension, and abduction.

Contralateral: On the opposite side.

Degree of Freedom: The movement of a joint in a plane.

Depression: The lowering movement of a body part such as the scapula.

Distal: A position relatively far from a designated reference point.

Dorsal: See Posterior.

Downward Rotation: The action whereby the scapula swings toward the midline of the body.

Dynamics: The branch of mechanics in which the system being studied undergoes acceleration.

Extension: The action in which the relative angle between two adjacent segments gets larger.

Frontal (Coronal) Plane: The plane that bisects the body into front and back halves.

Functional Anatomy: The study of the body components needed to achieve a human movement or function.

Hyperabduction: Abduction movement beyond the normal range of abduction.

Hyperadduction: Adduction movement beyond the normal range of adduction.

Hyperextension: Extension movement beyond the normal range of extension.

Hyperflexion: Flexion movement goes beyond the normal range of flexion.

Inferior: A position below a designated reference point.

Inversion: The movement in which the medial border of the foot lifts so that the sole of the foot faces away from the midline of the body.

Kinematics: Area of study that examines the spatial and temporal components of motion (position, velocity, acceleration).

Kinetics: Study of the forces that act on a system.

Lateral: A position relatively far from the midline of the body.

Lateral Flexion: A flexion movement of the head or trunk.

Linear Motion: Motion in a straight or curved line in which different regions of the same object move the same distance.

Longitudinal Axis: The axis through the center of mass of the body running from top to bottom.

Medial: A position relatively closer to the midline of the body.

Mediolateral Axis: The axis through the center of mass of the body running from right to left.

Movement or Motion: A change in place, position, or posture occurring over time and relative to some point in the environment.

Origin: The intersection of the axes of a reference system and the reference point from which measures are taken.

Plane of Motion: A two-dimensional surface running through an object. Motion occurs in the plane or parallel to the plane.

Posterior: A position behind a designated reference point.

Proximal: A position relatively closer to a designated reference point.

Qualitative Analysis: A nonnumeric description or evaluation of movement based on direct observation.

Quantitative Analysis: A numeric description or evaluation of movement based on data collected during the performance of the movement.

Reference System: A system to locate a point in space.

Relative Angle (Joint Angle): The included angle between two adjacent segments.

Relative Reference Frame: A reference frame in which the origin is at the joint center and one of the axes is placed along one of the segments.

Retraction: The motion describing the coming together action of the scapula.

Rotation: A movement about an axis of rotation in which not every point of the segment or body covers the same distance in the same time.

Sagittal Plane: The plane that bisects the body into right and left sides.

Statics: A branch of mechanics in which the system being studied undergoes no acceleration.

Transverse (Horizontal) Plane: The plane that bisects the body into top and bottom halves.

Superior: A position above a designated reference point.

Upward Rotation: The action whereby the scapula swings out from the midline of the body.

Upper limb (also upper extremity): in human anatomy, refers to the region distal to the deltoid. In formal usage, the term "arm" only refers to the structures from the shoulder to the elbow, explicitly excluding the forearm, and thus "upper limb" and "arm" are not synonymous. The upper limb includes the following structures: Shoulder Arm - in anatomy, the region between the shoulder and the elbow - Elbow, Forearm, Wrist, Hand